Neurotoxicology 75 (2019) 158–173

Contents lists available at ScienceDirect

Neurotoxicology

journal homepage: www.elsevier.com/locate/neuro

Structure-cytotoxicity relationship profile of 13 synthetic cathinones in differentiated human SH-SY5Y neuronal cells

Jorge Soares[a,*], Vera Marisa Costa[a], Helena Gaspar[b,c], Susana Santos[d,e], Maria de Lourdes Bastos[a], Félix Carvalho[a], João Paulo Capela[a,f,*]

[a] UCIBIO, REQUIMTE (Rede de Química e Tecnologia), Laboratório de Toxicologia, Departamento de Ciências Biológicas, Faculdade de Farmácia, Universidade do Porto, Portugal
[b] BioISI – Instituto de Biossistemas e Ciências Integrativas, Faculdade de Ciências, Universidade de Lisboa, Portugal
[c] MARE - Centro de Ciências do Mar e do Ambiente, Escola Superior de Turismo e Tecnologia do Mar, Instituto Politécnico de Leiria, Portugal
[d] Centro de Química e Bioquímica (CQB), Departamento de Química e Bioquímica, Faculdade de Ciências, Universidade de Lisboa, Portugal
[e] Centro de Química Estrutural, Faculdade de Ciências, Universidade de Lisboa, Portugal
[f] FP-ENAS (Unidade de Investigação UFP em Energia, Ambiente e Saúde), CEBIMED (Centro de Estudos em Biomedicina), Faculdade de Ciências da Saúde, Universidade Fernando Pessoa, Portugal

ARTICLE INFO

Keywords:
Synthetic cathinones
Classical amphetamines
Cytotoxicity
SH-SY5Y cells
Structure-toxicity relationship

ABSTRACT

Synthetic cathinones also known as β-keto amphetamines are a new group of recreational designer drugs. We aimed to evaluate the cytotoxic potential of thirteen cathinones lacking the methylenedioxy ring and establish a putative structure-toxicity profile using differentiated SH-SY5Y cells, as well as to compare their toxicity to that of amphetamine (AMPH) and methamphetamine (METH). Cytotoxicity assays [mitochondrial 3-(4,5-dimethyl-2-thiazolyl)-2,5-diphenyl-2H-tetrazolium bromide (MTT) reduction and lysosomal neutral red (NR) uptake] performed after a 24-h or a 48-h exposure revealed for all tested drugs a concentration-dependent toxicity. The rank order regarding the concentration that promoted 50 % of toxicity, at 24 h exposure, by the MTT assay was: 3,4-dimethylmethcathinone (3,4-DMMC) > METH > mephedrone ≈ α-pyrrolidinopentiophenone > AMPH ≈ methedrone > pentedrone > buphedrone ≈ flephedrone > α-pyrrolidinobutiophenone > methcathinone ≈ *N*-ethylcathinone > α-pyrrolidinopropiophenone > *N,N*-dimethylcathinone ≈ amfepramone. Apoptotic cell death signs were seen for all studied cathinones. 3,4-DMMC, methcathinone and pentedrone triggered autophagy activation, as well as increased reactive oxygen species production, and *N*-acetyl-L-cysteine (NAC) totally prevented that rise. Importantly, NAC was also able to prevent the cytotoxicity promoted by 6 tested drugs, ruling for an involvement of oxidative stress in the toxic events observed. The increased lipophilic chain on the alpha carbon, the presence and the high steric volume occupied by the substituents on the aromatic ring, and the substitution of the pyrrolidine ring by its secondary amine analogue have proved to be key points for the cytotoxicity profile of these cathinones. The structure-toxicity relationship established herein may enlighten future human relevant mechanistic studies, and future clinical approaches on intoxications.

1. Introduction

Synthetic cathinones are chemical analogues of the naturally occurring cathinone, which can be found in the fresh leaves and stems of the *Catha edulis* (khat) plant (Katz et al., 2014; Thornton and Baum, 2014). These designer drugs have emerged in the market in the mid-2000's and their use has been massively increasing, especially among adolescents and young adults, as they are inexpensive and readily available in smartshops and online (EMCDDA, 2018; Kelly, 2011; Prosser and Nelson, 2012). Producers marketed this class of new psychoactive substances with very appealing names, such as "Vanilla Sky", "Ivory Wave" or "Meow-meow", and eye-catching packaging. They are sold as "bath salts" or "plant food" and labelled "not for human consumption" in an attempt to circumvent the law (Olives et al., 2012; Valente et al., 2014; Weaver et al., 2015). By introducing small chemical modifications in the basic structure of previous drugs, several derivatives are placed in the market every year, dodging the regulation of the law enforcement agencies (Albertson, 2014; Mas-Morey et al.,

* Corresponding authors at: UCIBIO, REQUIMTE, Laboratório de Toxicologia, Faculdade de Farmácia, Universidade do Porto, Rua de Jorge Viterbo Ferreira, 228, 4050-313, Porto, Portugal.
E-mail addresses: jorge.emt.soares@gmail.com (J. Soares), joaoc@ufp.edu.pt (J.P. Capela).

https://doi.org/10.1016/j.neuro.2019.08.009
Received 24 November 2018; Received in revised form 30 July 2019; Accepted 21 August 2019
Available online 29 August 2019
0161-813X/

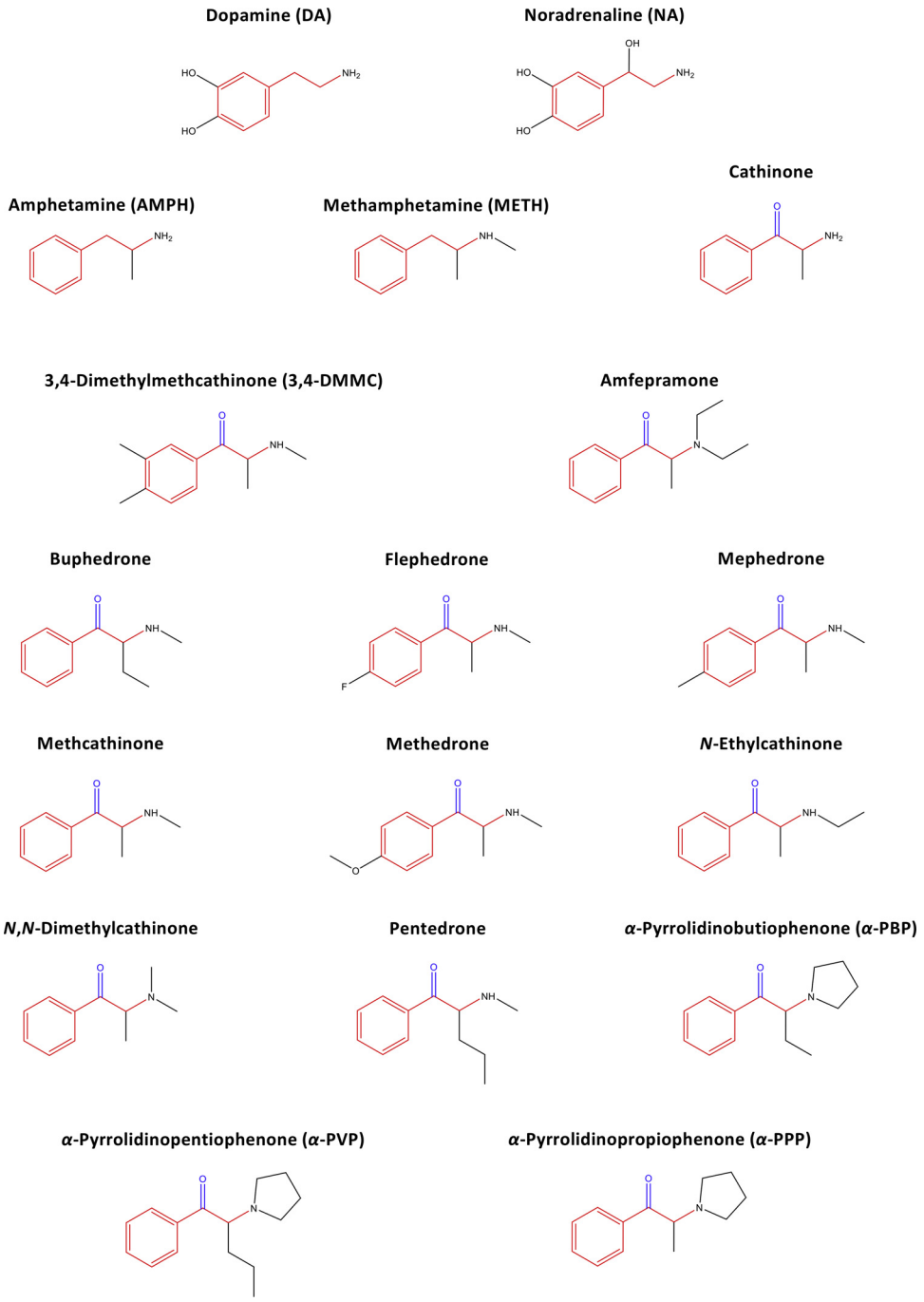

Fig. 1. Chemical structures of synthetic cathinones [3,4-dimethylmethcathinone (3,4-DMMC), amfepramone, buphedrone, flephedrone, mephedrone, methcathinone, methedrone, *N*-ethylcathinone, *N,N*-dimethylcathinone, pentedrone, *α*-pyrrolidinobutiophenone (*α*-PBP), *α*-pyrrolidinopentiophenone (*α*-PVP) and *α*-pyrrolidinopropiophenone (*α*-PPP)]. Classical amphetamines [amphetamine (AMPH) and methamphetamine (METH)] and the monoamine neurotransmitters [dopamine (DA) and noradrenaline (NA)] have a phenethylamine group (placed in red) as a common structure. The synthetic cathinones differ from the classic structure of amphetamine by presenting a keto group (placed in blue) at position β to the nitrogen atom (For interpretation of the references to colour in this figure legend, the reader is referred to the web version of this article).

2013; Stiles et al., 2016). Since their appearance, the number of cathinones seizures has been increasing exponentially, a pattern that points to the considerable demand for these designer drugs. In 2017, the European Union Early Warning System identified 51 new psychoactive substances, of which 12 were synthetic cathinones making them the second largest class of new psychoactive substances in Europe. Actually, before that, the synthetic cathinones were leading the ranking of the so-called “legal” drugs, reported for the first time, for 3 years in a row (EMCDDA, 2018).

Synthetic cathinones are closely related to phenethylamines, like amphetamine (AMPH), methamphetamine (METH) or 3,4-methylenodioximethamphetamine (ecstasy), from which they differ by the presence of a keto group at β position to the nitrogen atom (see Fig. 1), for this reason being seldom named β-keto amphetamines. Therefore, it is to be expected that cathinones share similar pharmacological effects with amphetamine-related drugs (Valente et al., 2017a). In fact, several studies demonstrated that synthetic cathinones stimulate the release of neurotransmitters such as dopamine (DA), noradrenaline (NA) and serotonin (5-hydroxytryptamine, 5-HT) and/or inhibit their reuptake (Baumann et al., 2012; Kolanos et al., 2015; Simmler et al., 2013). It is possible to divide synthetic cathinones into two major groups: those closer to AMPH-related pharmacological activities, lacking the methylenedioxy ring, and those closer to ecstasy, bearing the methylenedioxy ring (Gunderson et al., 2013; Valente et al., 2014).

Subjective effects reported by cathinones users include increased empathy and energy, sexual arousal and social opening feelings (Mas-Morey et al., 2013). Although they are usually advertised as safe, these drugs were found to cause several adverse effects, such as agitation, tachycardia, hallucinations, nausea and vomiting, dizziness and increased sweating, hyperthermia, depression and death (Mas-Morey

et al., 2013; Stiles et al., 2016; Watterson and Olive, 2014; Weaver et al., 2015).

Despite the numerous synthetic cathinones available in the market, recent data showed that mephedrone remains one of the most consumed drug (EMCDDA, 2018). An young adult presented numerous psychotic symptoms, as paranoid delusions, intense anxiety and visual and kinaesthetic hallucinations, after intravenous injections of mephedrone regularly for 4 months (Dolengevich-Segal et al., 2016). In fact, anxiety, hallucinations, delusions, paranoia, seizures and psychosis were the main neurologic/psychiatric effects related to mephedrone use (German et al., 2014; Wood and Dargan, 2012). Other reports point to the potential neurotoxic effects of these compounds in humans (Boulanger-Gobeil et al., 2012; Marinetti and Antonides, 2013; Rojek et al., 2016; Thornton et al., 2012; Zuba et al., 2013). Those effects can be explained since synthetic cathinones can act both as substrates or inhibitors of monoamine transporters (Zwartsen et al., 2017). For instance, mephedrone is a releasing agent with additional reuptake blocking properties, acting as a DA transporter (DAT) substrate at low micromolar concentrations, whereas α-pyrrolidinopentiophenone (α-PVP) is a potent reuptake blocking agent, acting thereby as a DAT and NA transporter inhibitor at nanomolar concentrations. Moreover, the effective concentrations of most reported cathinones, at monoamine transporters, are in line with those estimated for the human brain, generally in low micromolar range (0.001–36 μM). Nonetheless, other targets, as monoamine receptors, are less relevant since the reported concentrations required to produce the cathinones harmful effects are higher (e.g. mephedrone's binding affinity for dopamine receptors is greater than 10 μM) (Hondebrink et al., 2018). The reviewed findings revealed the monoamine transporters and receptors as the putative main targets of cathinones for their elicited neurotoxic effects in humans.

Few studies were conducted in laboratory settings for these drugs, but among those, mephedrone has proven its neurotoxic potential. Mephedrone seems to induce loss of DA transporters in the frontal cortex and 5-HT transporters in the frontal cortex, striatum and hippocampus of adolescent rats after subcutaneous (s.c.) administration of 3 x 25 mg/Kg per day (every 2 h), for 2 days (Lopez-Arnau et al., 2015). Martinez-Clemente et al. (2014) have reported a reduction of monoamine transporters in frontal cortex and hippocampus of mice after administration of 25 or 50 mg/Kg mephedrone (s.c.). Meanwhile, the few *in vitro* studies that exist usually focus on a small number of cathinones. The study presented herein aimed to ascertain the cytotoxicity of thirteen synthetic cathinones lacking the methylenedioxy ring, namely 3,4-dimethylmethcathinone (3,4-DMMC), amfepramone, buphedrone, flephedrone, mephedrone, methcathinone, methedrone, *N*-ethylcathinone, *N,N*-dimethylcathinone, pentedrone, α-pyrrolidinobutiophenone (α-PBP), α-pyrrolidinopropiophenone (α-PPP) and α-PVP (Fig. 1), to compare their effects to the classical drugs AMPH and METH, using a neuronal dopaminergic human cell culture model (differentiated SH-SY5Y cells). Moreover, with such a broad number of drugs studied, a putative structure-toxicity profile for these new psychoactive compounds was tentatively drawn.

2. Material and methods

2.1. Chemicals and materials

The synthesis or isolation of all cathinones used in this work was carried out under the protocol established between the Faculty of Sciences of the University of Lisbon, the Forensic Science Laboratory from Portuguese Criminal Police and the Faculty of Pharmacy of the University of Porto. Nine cathinones without the methylenedioxy ring (amfepramone, buphedrone, mephedrone, methcathinone, *N,N*-dimethylcathinone, pentedrone, α-PBP, α-PPP and α-PVP) were previously synthetized as their corresponding hydrochloride salts with a purity higher than 97 %, and their characterization was reported in a previous paper (Gaspar et al., 2018); 3,4-DMMC, flephedrone, methedrone and *N*-ethylcathinone came from Portuguese smartshops and were supplied by the Forensic Science Laboratory from Portuguese Criminal Police.

Dulbecco's modified Eagle's medium (DMEM) high glucose, sodium bicarbonate, trypan blue solution 0.4 % (w/v), trypsin-EDTA solution, retinoic acid (RA), 12-*O*-tetradecanoylphorbol-13-acetate (TPA), 3-(4,5-dimethyl-2-thiazolyl)-2,5-diphenyl-2H-tetrazolium bromide (MTT), 3-amino-7-dimethylamino-2-methylphenazine hydrochloride (neutral red or NR), *N*-acetyl-L-cysteine (NAC), 4,5-dihydroxy-1,3-benzenedisulfonic acid disodium salt (tiron), 3-[2-(3,5-dimethyl-2-oxocyclohexyl)-2-hydroxyethyl]glutarimide (cycloheximide or CHX), Hoechst 33258 stain solution, 2′,7′-dichlorodihydrofluorescein diacetate (DCFH-DA), *tert*-butyl hydroperoxide solution (Luperox® TBH70X) and METH were obtained from Sigma-Aldrich (Germany). Threo-methyl-α-phenyl-2-piperidineacetate hydrochloride (methylphenidate or MPH) and AMPH were obtained from Tocris (United Kingdom). CYTO-ID® autophagy detection kit was obtained from ENZO (United Stated of America). Antibiotic mixture (10 000 U mL^{-1} penicillin, 10 000 μg mL^{-1} streptomycin) was obtained from Biochrom (Germany). 3-Methyladenine (3-MA) was obtained from Abcam (United Kingdom). Heat inactivated foetal bovine serum (FBS), Hanks' balanced salt solution (HBSS) and phosphate buffer solution with calcium and magnesium [PBS (+/+)] were obtained from Gibco (United Kingdom). All sterile plastic material was obtained from Corning Costar (United States of America).

2.2. Characterization and purity evaluation of cathinones

Samples of 4 different packs from smartshop products - "Bliss", "Blast", "Space Invader E.T"-pack 1, "Space invader"-pack 2 - containing methedrone, flephedrone, 3,4-DMMC and *N*-ethylcathinone, respectively, were characterized through several analytical techniques [(Nuclear Magnetic Resonance (NMR), Gas Chromatography - Mass Spectrometry (GC—MS) and Ion Chromatography (IC)] and their purity assessed by the methodology previously described for other cathinones (Gaspar et al., 2015). Briefly, an aliquot of each cathinone (10 to 15 mg) was dissolved in dimethylsulfoxide (DMSO)-d_6 to run NMR structural analysis and in deuterated water (D_2O) for qNMR quantification. ^1H NMR (400.1 MHz), ^{13}C NMR (100.6 MHz) were recorded on a Bruker Avance spectrometer; chemical shifts were expressed as δ values and referenced to the residual solvent peak (DMSO- d_6, δH = 2.50, δC = 39.5) and coupling constants were reported in units of Hertz (Hz). Unequivocal assignments of all proton and carbon signals was achieved by 1D (^1H, ^{13}C, APT) and 2D (COSY, HMBC and HSQC) NMR experiments. For purity evaluation, each sample (*ca.* 10 mg) was dissolved in 500 μL of a standard solution of maleic acid (CRM for quantitative NMR, Fluka, purity 99 %) in D_2O with a concentration of 10 mg/mL. The proton chemical shifts were calculated using as reference the maleic acid resonance signal at 6.42 ppm. The ^1H signal integration for each compound (methedrone CH_3 at δ3.94 ppm; flephedrone CH_3 at δ2.83 ppm; 3,4-DMMC CH_3 at δ2.88 ppm and *N*-ethylcathinone CH_3 at δ1.63 ppm) was calculated calibrating for 100 the area of maleic acid resonance peak. The absolute quantity (mol) was determined through the ratio between the integration of the target protons of each compound and the signal of maleic acid. The purity of all the cathinones was found to be higher than 97 % except for flephedrone which was contaminated with caffeine. Successive recrystallizations with mixtures of methanol/diethyl ether enabled elimination of caffeine and the obtention of flephedrone with a purity > 98 %. The purity of the cathinones (≥ 97 %) was also confirmed by GC—MS analysis using an Agilent® GC system 7890B series coupled with a MSD Agilent® 5977B [HP-5MS coated capillary column (30 m x 250 μm x 0.25 μm)] using helium as carrier gas with a flow of 1 mL/min. Samples were dissolved in methanol/dichloromethane 1:1 and 1 μL of the solution was injected in split mode 100:1. The GC oven was programmed at 80 °C (1 min),

heated at a rate of 12 °C/min to 270 °C (7 min). The injector temperature was 230 °C and the GC−MS transfer line temperature was 150 °C. Electron ionization (EI) energy was 70 eV. Scan range was 40–250 m/z. The analysis of the aqueous solution of all cathinones by IC as described elsewhere (Gaspar et al., 2015), allowed to confirm that they were all in their hydrochloride salts. The NMR data obtained for *N*-ethylcathinone and 3,4-DMMC in DMSO were similar to the previously reported data (Gaspar et al., 2018; McDermott et al., 2011). For flephedrone and methedrone the NMR data were consistent with the literature data in different NMR solvents (Alotaibi et al., 2015; Araujo et al., 2015; Archer, 2009) and with the published spectra in DMSO (Nic Daeid et al., 2014). The full ^{1}H and ^{13}C NMR assignments for these two cathinones in DMSO are reported here for the first time.

3,4-DMMC: ^{1}H NMR (400 MHz, DMSO-d_6) δ 9.45 (2H, *brs*, NH_2), 7.83 (1H, *brs*, H-2'), 7.77 (1H, *d*, *J* = 7.8 Hz, H-6'), 7.37 (1H, *d*, *J* = 7.8 Hz, H-5'5'), 5.12 (1H, *m*, H-2), 2.56 (3H, s, *N*−CH_3), 2.31 (6H, s, CH_3-C3'/CH_3-C4'), 1.43 (3H, *d*, *J* = 7.1 Hz, H-3). ^{13}C NMR (100 MHz, DMSO-d_6) δ 196.02 (C = O, C-1), 144.35 (Cq, C-4'), 137.46 (Cq, C-3'), 130.80 (Cq, C-1'), 130.18 (CH, C-5'), 129.60 (CH, C-2'), 126.54 (CH, C-6'), 58.08 (CH, C-2), 30.61 (*N*-CH_3), 19.75 (CH_3-C4'), 19.30 (CH_3-C3'), 15.62 (CH_3, C-3).

Flephedrone: ^{1}H NMR (400 MHz, DMSO-d_6) δ 9.33 (1H, *brs*, NH), 8.36 (2H, *dd*, *J* = 8.4, 2.2 Hz, H-2'/H-6'), 7.45 (2H, *t*, *J* = 8.7 Hz, H-3'/H-5'), 5.19 (1H, *q*, *J* = 7.1 Hz, H-2'), 2.59 (3H, *brs*, *N*-CH−CH_3), 1.44 (3H, *d*, *J* = 7.1 Hz, H-3'), ^{13}C NMR (100 MHz, DMSO-d_6) δ 195.08 (C = O, C-1), 165.87 (C–F, *d*, *J* = 254 Hz, C-4'), 132.11 (CH, *d*, *J* = 9.9 Hz, C-2'), 129.71 (Cq, *d*, *J* = 3.5 Hz, C-1'), 116.46 (CH, *d*, *J* = 22.3 Hz, C-3'), 58.26 (CH, C-2), 30.71 (*N*−CH_3), 15.34 (CH_3, C-3).

Methedrone: ^{1}H NMR (400 MHz, DMSO-d_6) δ 9.66 (1H, *brs*, *N*H), 9.16 (1H, *brs*, *N*H), 8.02 (2H, *d*, *J* = 8.9 Hz, H-2'/H-6'6'), 7.12 (2H, *d*, *J* = 8.9 Hz, H-3'/H-5'), 5.19 (1H, *m*, H-2'), 3.87 (3H, *s*, O−CH_3), 2.56 (3H, *brs*, *N*-CH−CH_3), 1.44 (3H, *d*, *J* = 7.1 Hz, H-3'); ^{13}C NMR (100 MHz, DMSO-d_6) δ 194.59 (C = O, C-1), 164.30 (Cq, C-4'), 131.38 (CH, C-2'), 125.70 (Cq, C-1'), 114.50 (CH, C-3'), 57.87 (CH, C-2), 55.84 (O−CH_3), 30.68 (*N*−CH_3), 15.77 (CH_3, C-3).

N-Ethylcathinone: ^{1}H NMR (400 MHz, DMSO-d_6) δ 9.47 (2H, *brs*, NH_2), 8.07 (2H, *d*, *J* = 7.5 Hz, H2'/H-6'), 7.75 (1H, t, *J* = 7.4 Hz, H-4'), 7.61 (2H, t, *J* = 7.7 Hz, H-3'/H-5'), 5.22 (1H, *m*, H-2), 3.04 (1H, *m*, *N*−CH_2CH_3, H_a), 2.92 (1H, *m*, *N*−CH_2CH_3, H_b), 1.47 (3H, *d*, *J* = 7.1 Hz, H-3), 1.27 (3H, t, *J* = 7.2 Hz, *N*−CH_2CH_3); ^{13}C NMR (100 MHz, DMSO-d_6) δ 196.36 (C = O, C-1), 134.73 (CH, C-4'), 132.94 (Cq, C-1'), 129.22 (CH, C-3'/C-5') 128.87 (CH, C-2'/C-6'), 56.73 (CH, C-2), 40.31 (CH_2, *N*−CH_2), 15.68 (CH_3, C-3), 11.20 (CH_3, *N*−CH_2CH_3).

2.3. Cell culture and differentiation

SH-SY5Y cells were used to perform the cytotoxicity studies. Human neuroblastoma cells, SH-SY5Y, (ATCC, United States of America) were cultured in 25 cm^2 flasks using complete medium (DMEM supplemented with 10 % FBS, 100 U mL^{-1} of penicillin and 100 μg mL^{-1} of streptomycin). Cells were incubated at 37 °C in a humidified 5 % CO_2-95 % air atmosphere until confluence. SH-SY5Y cells were trypsinized (trypsin/EDTA) and the cell suspension was counted before seeding in 48-well plates at the density of 25 000 cells/cm^2. In order to attain the dopaminergic neuronal phenotype, with cells exhibiting high levels of DAT and tyrosine hydroxylase, SH-SY5Y cells were then differentiated as described previously (Barbosa et al., 2014; Ferreira et al., 2013). For the differentiation protocol, SH-SY5Y cells were seeded in complete DMEM medium containing 10 μM RA, and cultured for 3 days. Complete medium containing 80 nM TPA was then added to each well and cells were maintained for another 3 days. In all experiments, cells were used between passages 23 and 31.

2.4. Drug exposure

Following the differentiation protocol, the medium was removed and replaced with fresh complete DMEM medium. Cells were then acutely exposed to AMPH, METH, 3,4-DMMC, amfepramone, buphedrone, flephedrone, mephedrone, methcathinone, methedrone, *N*-ethylcathinone, *N,N*-dimethylcathinone, pentedrone, *α*-PBP, *α*-PPP or *α*-PVP for 24 h or 48 h at 37 °C and 5 % CO_2. A wide concentration range (0.25–20 mM) was studied for each drug in order to obtain a concentration-toxicity curve at 24 h of exposure. Stock solutions of all synthetic cathinones were made in sterile water and stored at -20 °C. In order to avoid any effect of the solvent, the control wells were exposed to the same volume of sterile water as that used for the drug-treated wells.

2.5. Cytotoxicity assays

The cytotoxicity assays, MTT reduction and NR uptake, were performed in differentiated SH-SY5Y cells and will be briefly described.

2.5.1. MTT reduction assay

The MTT reduction is mainly done by mitochondrial dehydrogenases and therefore this assay can be seen as a measure of mitochondrial dysfunction (Capela et al., 2007b; Costa et al., 2009). After a 24-h or 48-h exposure period, the medium of each well was removed and replaced by fresh DMEM medium containing 500 μg mL^{-1} MTT. Then, the cells were incubated at 37 °C, 5 % CO_2 for 3 h, after which the medium was removed and DMSO was added. The plates were stirred for 15 min and then the amount of formazan formed was measured at 550 nm in a multi-well plate reader (Biotek Instruments, United States of America). The percentage of MTT reduction of control cells was set to 100 % in each experiment (Barbosa et al., 2014), and the effects of the tested compounds are expressed as the percentage of control cells at the same time-point.

2.5.2. NR uptake assay

The NR uptake assay assesses the capability of live cells to incorporate NR into their lysosomes, and was performed as previously described (Reis-Mendes et al., 2017). After the incubation period, the medium was replaced by fresh medium containing 33 μg mL^{-1} NR, and cells were incubated at 37 °C, 5 % CO_2 for 3 h. The medium was then removed and cells were washed with a warmed solution of HBSS with calcium and magnesium. A 50 % ethanol/1 % glacial acetic acid solution was then used to promote lysis of the incubated cells and dissolve the intracellular NR. The absorbance was measured at 540 nm and 690 nm (the reference wavelength) in a multi-well plate reader (Biotek Instruments, United States of America). Results were expressed in percentage of control wells in each experiment, whose mean values were set to 100 %.

2.6. Neuroprotection experiments

2.6.1. MTT reduction assay

Cells were pre-treated with 1 mM NAC (Capela et al., 2006), 100 μM tiron (Ferreira et al., 2013), 10 nM CHX (Martins et al., 2013), 1 μM MPH (Ludolph et al., 2006) or 1 mM 3-MA (Zhang et al., 2018), 30 min before adding the tested drugs at a concentration that promoted 50 % of lethality (LC_{50}) when evaluated by the MTT assay at 24 h. Of note, the putative neuroprotective compounds were not removed. Then, cells were incubated for 24 h at 37 °C and 5 % CO_2, after which the MTT reduction assay was carried out as described above.

2.6.2. Reactive oxygen species (ROS) production

In order to give further insights on the involvement of oxidative stress, the production of intracellular levels of ROS was assessed using the DCFH-DA probe, after cells exposure to LC_{50} of 3,4-DMMC, methcathinone, pentedrone or AMPH (Valente et al., 2017b), in the presence or absence of NAC. Briefly, following the differentiation protocol, cells were simultaneously pre-incubated with DCFH-DA (10 μM) and NAC (1

mM), at 37 °C, 5 % CO_2 for 30 min. The medium was then removed and cells were exposed to the drugs alone, or with NAC. Then, the fluorescence ($\lambda_{excitation\ maximum}$ = 485 nm and $\lambda_{emission\ maximum}$ = 530 nm) was measured at 6 and 24 h after exposure to the drugs, in a multi-well plate reader (Biotek Instruments, United States of America). Of note, 150 μM Luperox® TBH70X (a ROS inducer agent) was used as positive control for ROS production. Also, only these compounds (3,4-DMMC, methcathinone, pentedrone and AMPH) were used, since we add no more availability of the remaining.

2.7. Microscopic evaluation of the cells

2.7.1. Phase-contrast microscopy

Morphological changes in SH-SY5Y differentiated cells after a 24-h exposure period to the LC_{50}, previously calculated by the data obtained in the MTT reduction assay at 24 h of AMPH, METH or synthetic cathinones, were assessed by capturing phase-contrast microphotographs in a Nikon Eclipse TS100 equipped with a Nikon DS-Fi1 camera (Japan).

2.7.2. Hoechst nuclear staining

In order to assess alterations in cellular nuclear morphology, microphotographs were taken from exposed cells stained with Hoechst 33258 after exposure to the LC_{50} calculated by the data obtained in the MTT reduction assay at 24 h incubation. Hoechst 33258 dye solution stains DNA, and by doing so allows to distinguish condensed chromatin and nuclear fragmentation, both characteristic features of apoptotic cell death (Prokhorova et al., 2015). After binding to DNA, Hoechst dye emits blue fluorescence (Valente et al., 2016). The protocol was done as follows: after a 24-h exposure period, the medium was removed, and cells were fixed by adding paraformaldehyde 4 % for 10 min at 4 °C. Then, paraformaldehyde was removed, and cells were rinsed twice with PBS (+/+). Cells were incubated with Hoechst 33258 (5 μg mL^{-1}) solution at 37 °C, 5 % CO_2 for 10 min while protected from light. Cells were then rinsed with PBS (+/+) and photographed with a microscope equipped with a fluorescent filter ($\lambda_{excitation\ maximum}$ = 346 nm and $\lambda_{emission\ maximum}$ = 460 nm) (Nikon Eclipse TS100 equipped with a Nikon DS-Fi1 camera, Japan) (Reis-Mendes et al., 2017).

2.7.3. Autophagy activation

Autophagy is a complex process in which damaged proteins, and even entire organelles, are surrounded by a double-membrane vesicle, called autophagosome, which in turn fuses with a lysosome (autolysosome), the internal material being digested. Under certain stress stimuli, as drug exposure, autophagy can be activated (Chan et al., 2012). Drug-induced autophagic activity in differentiated SH-SY5Y cells exposed for 24 h to the LC_{50} (calculated by the data obtained in the MTT reduction assay, at 24 h incubation) of synthetic cathinones (3,4-DMMC, methcathinone and pentedrone) and AMPH was evaluated using the CYTO-ID® autophagy detection kit. After the exposure period, cells were trypsinized and centrifuged at 1 200 rpm for 5 min. Cells were then washed with PBS (+/+) and centrifuged again. Afterwards, cells were re-suspended in 100 μL of diluted CYTO-ID® green stain solution (1 μL of CYTO-ID® green detection reagent in 1 mL of 1x assay buffer) and incubated for 30 min, at room temperature in the dark. Samples were then analysed using a BD Accuri™ C6 flow cytometer (BD Biosciences, United States of America), using the green (FL1) channel. In each sample, a minimum of 20 000 events were acquired for analysis. Data were analysed using BD Accuri™ software. Of note, 500 nM rapamycin (a well-established autophagy inducer) and 10 μM chloroquine (an inhibitor of lysosomal activity) were used alone or in combination, as positive controls, as recommended by the manufacturer. Also, only these compounds (3,4-DMMC, methcathinone, pentedrone and AMPH) were used, since we add no more availability of the remaining.

2.8. Statistical analysis

Data were presented as mean ± standard deviation (SD), being the LC_{50} data the only exception which were presented as mean and 95 % confidence interval (CI 95 %). D'Agostino & Pearson omnibus test was used in order to assess if data followed a normal distribution. One-way ANOVA or in the case of data concerning ROS production two-way ANOVA with repeated measures were used to compare means of different treatment groups, followed by the Tukey or Sidak, respectively, post hoc test. For each drug, the LC_{50} values were obtained by analysis of the MTT and NR dose-response curves. Curves were fitted using least squares as the fitting method, and the comparisons between curves (LC_{50}) were made using the extra sum-of-squares *F* test. More details of the statistical analysis are provided in the legend of the figures and table. Statistical significance was considered for p values < 0.05. All statistical analysis was performed using the GraphPad Prism 6 software (United States of America).

3. Results

3.1. Synthetic cathinones lacking the methylenedioxy ring induced a concentration-dependent cytotoxicity

The cytotoxic profile of cathinones was analysed through the MTT reduction and NR uptake assays (performed at 24 and 48 h). The data obtained were compared to that of classical amphetamines, AMPH and METH. Results are displayed in Fig. 2 (data obtained for the earlier time-point regarding MTT reduction), Supplementary Fig. 1 (data obtained for the earlier time-point regarding NR uptake) and Table 1 (data obtained for both time-points) by alphabetic order, first the classical amphetamines, followed by the synthetic cathinones.

According to the MTT reduction assay, after a 24-h exposure, *α*-PBP and *α*-PVP induced significant cytotoxicity for all tested concentrations, when compared to control cells (deionized sterile water incubated) as depicted in Fig. 2m and 2o, respectively. Similarly, mephedrone (Fig. 2g) also exhibited significant toxicity for the lowest tested concentration (0.25 mM), however it only caused significant cytotoxicity again at concentrations 2.5 mM and 5 mM. Buphedrone (Fig. 2e), flephedrone (Fig. 2f), methcathinone (Fig. 2h) and *N,N*-dimethylcathinone (Fig. 2k) showed significant cytotoxicity for all tested concentrations equal to or above 0.5 mM, when compared to control cells, at the 24-h time-point. Of note, as the four previously mentioned drugs, methedrone (Fig. 2i) induced significant cytotoxicity for the concentration of 0.5 mM. Nonetheless, it lacks significant toxicity for 1 mM concentration, leading to a significant decrease in MTT reduction again for the highest concentrations tested (2.5 and 5 mM). METH (Fig. 2b), and the synthetic cathinones 3,4-DMMC (Fig. 2c) and *α*-PPP (Fig. 2n) caused significant cytotoxicity for all concentrations equal to or above 1 mM, when compared to control cells, after a 24-h exposure. In the same line, amfepramone exhibited significant cytotoxicity at the 1 mM concentration, although it only induced significant cytotoxicity again at concentrations equal to or above 5 mM, as depicted in Fig. 2d. At the 24-h time-point, pentedrone (Fig. 2l) and AMPH (Fig. 2a) exhibited significant cytotoxicity, when compared to control cells, for all concentrations equal to or above 2 and 2.5 mM, respectively, while *N*-ethylcathinone (Fig. 2j) caused significant cytotoxicity in the concentration range of 5–20 mM.

In the NR uptake assay, 3,4-DMMC presented the highest cytotoxic effect (concentrations ≥ 1.5 mM) for 24 h of exposure, as depicted in Supplementary Fig. 1c. Pentedrone (Supplementary Fig. 1l) exhibited significant toxicity for all tested concentrations equal to or above 2 mM, when compared to control cells. Two and a half mM was the lowest concentration at which AMPH (Supplementary Fig. 1a), METH (Supplementary Fig. 1b), mephedrone (Supplementary Fig. 1g) and *α*-PVP (Supplementary Fig. 1o) exerted significant cytotoxicity, when compared to control cells. However, twice the concentration (5 mM)

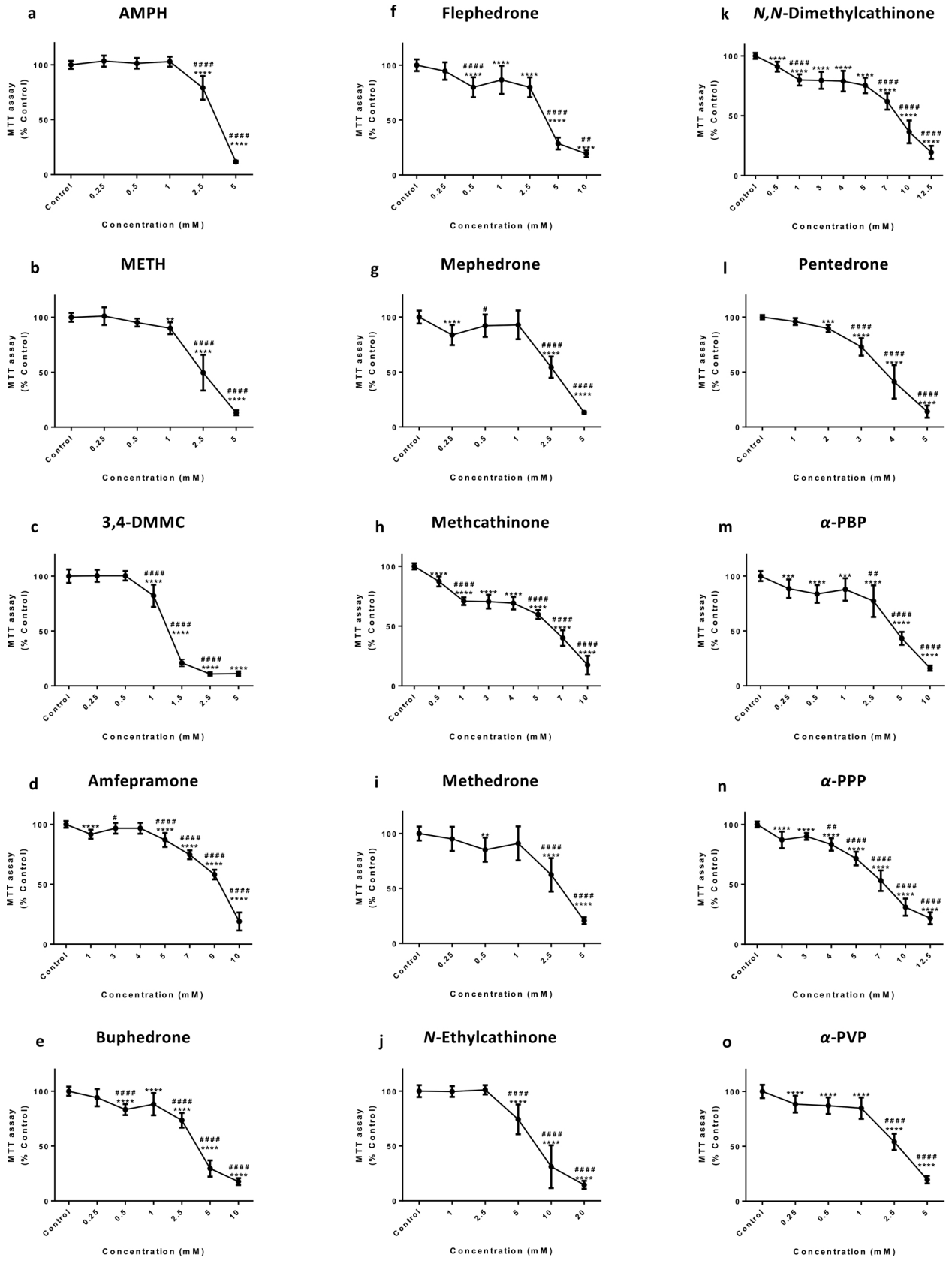

Fig. 2. Mitochondrial dysfunction in neuronal differentiated SH-SY5Y cells assessed by the MTT reduction assay. MTT assay was performed after a 24-h exposure. Data in percentage of control are presented as mean ± SD. Statistical analyses were performed using one-way ANOVA, followed by the Tukey's post hoc test (from at least 5 independent experiments performed in quadruplicate) ($^{**}p < 0.01$, $^{***}p < 0.001$, $^{****}p < 0.0001$ concentration vs. control; $^{\#}p < 0.05$, $^{\#\#}p < 0.01$, $^{\#\#\#\#}p < 0.0001$ concentration vs. previous concentration).

Table 1
LC_{50} after a 24- or 48-h exposure obtained by analysis of MTT and NR concentration-response curves. Curves were fitted using least squares as the fitting method, and the statistical comparisons between curves (LC_{50}) concerning the both tested time-points were made using the extra sum-of-squares *F* test (*$p < 0.05$, **$p < 0.01$, ***$p < 0.001$, ****$p < 0.0001$ 24-h time-point vs. 48-h time-point; n.a. not available). The LC_{50} data in bold are referred to the means values. Data, as mean and CI 95 %, are presented in mM.

	LC_{50} - Mean (CI 95 %)			
	MTT reduction assay		NR uptake assay	
	24 h	48 h	24 h	48 h
AMPH	**3.23** (3.13 to 3.34)	**2.85** (2.69 to 3.02)***	**2.98** (2.80 to 3.16)	**3.39** (3.19 to 3.59)**
METH	**2.48** (2.33 to 2.65)	**2.82** (2.66 to 3.00)**	**3.20** (2.98 to 3.44)	**3.57** (3.32 to 3.83)*
3,4-DMMC	**1.24** (1.21 to 1.27)	**1.43** (1.36 to 1.51)****	**1.34** (1.30 to 1.37)	**1.59** (1.49 to 1.69)****
Amfepramone	**9.29** (9.20 to 9.37)	**7.23** (7.04 to 7.42)****	**8.72** (8.14 to 9.35)	**6.45** (5.96 to 6.98)****
Buphedrone	**4.16** (3.88 to 4.46)	**3.54** (3.28 to 3.82)**	**7.97** (5.94 to 10.70)	**7.42** (4.92 to 11.21)
Flephedrone	**4.41** (4.06 to 4.78)	**3.75** (3.52 to 3.99)**	**6.74** (5.08 to 8.94)	**7.44** (4.98 to 11.14)
Mephedrone	**2.87** (2.69 to 3.05)	**2.19** (2.02 to 2.38)****	**3.27** (3.09 to 3.46)	**2.66** (2.50 to 2.84)****
Methcathinone	**6.21** (5.21 to 7.40)	**5.21** (3.78 to 7.20)	**6.29** (6.08 to 6.50)	**5.79** (5.59 to 6.00)**
Methedrone	**3.27** (3.01 to 3.55)	**2.76** (2.52 to 3.02)**	**4.41** (3.99 to 4.88)	**3.05** (2.90 to 3.21)****
***N*-Ethylcathinone**	**7.39** (6.75 to 8.09)	**6.03** (5.55 to 6.55)***	**8.31** (7.43 to 9.30)	**9.02** (7.74 to 10.50)
***N,N*-Dimethylcathinone**	**8.46** (7.11 to 10.07)	**5.59** (4.22 to 7.40)**	**9.07** (8.78 to 9.38)	**6.75** (6.49 to 7.01)****
Pentedrone	**3.77** (3.67 to 3.87)	**2.71** (2.62 to 2.81)****	**2.99** (2.86 to 3.12)	**2.34** (2.22 to 2.47)****
α-PBP	**5.15** (4.81 to 5.52)	**4.42** (4.16 to 4.68)[n.a.]	**6.07** (4.72 to 7.81)	**4.74** (3.27 to 6.86)
α-PPP	**8.06** (7.78 to 8.36)	**5.89** (5.68 to 6.11)****	**8.93** (8.56 to 9.32)	**5.37** (5.03 to 5.74)****
α-PVP	**3.01** (2.84 to 3.19)	**2.35** (2.14 to 2.58)****	**3.44** (3.28 to 3.61)	**2.66** (2.52 to 2.80)****

was required to cause significant toxicity for 6 of the 15 tested drugs: amfepramone (Supplementary Fig. 1d), buphedrone (Supplementary Fig. 1e), flephedrone (Supplementary Fig. 1f), methcathinone (Supplementary Fig. 1h), methedrone (Supplementary Fig. 1i) and α-PBP (Supplementary Fig. 1m). *N,N*-Dimethylcathinone (Supplementary Fig. 1k) and α-PPP (Supplementary Fig. 1n) began exhibiting significant cytotoxicity, when compared to control cells, for concentrations equal to or above 7 mM, while 10 mM of *N*-ethylcathinone (Supplementary Fig. 1j) was required to trigger lysosomal impairment in this model assay, at the 24-h time-point.

3.2. 3,4-DMMC was the most toxic tested compound, presenting the lowest LC_{50} value

LC_{50} values for both cytotoxicity assays were calculated through analysis of the fitted concentration-toxicity curves, at 24 and 48 h exposure. LC_{50} value represents the concentration at which each compound induces 50 % of lethality. Calculated values are presented in Table 1, for the two tested time-points.

For the MTT reduction assay at 24 h (Table 1), the calculated LC_{50} values pointed 3,4-DMMC (1.24 mM) as the most cytotoxic of all drugs under study, being more toxic than METH (2.48 mM) and AMPH (3.23 mM), followed by mephedrone (2.87 mM), α-PVP (3.01 mM), methedrone (3.27 mM), pentedrone (3.77 mM), buphedrone (4.16 mM), flephedrone (4.41 mM), α-PBP (5.15 mM), methcathinone (6.21 mM), *N*-ethylcathinone (7.39 mM), α-PPP (8.06 mM), *N,N*-dimethylcathinone (8.46 mM) and amfepramone (9.29 mM). Similarly, 3,4-DMMC presented the lowest LC_{50} value in the MTT test after 48 h (1.43 mM), while amfepramone proved to be the least toxic compound, presenting a LC_{50} value of 7.23 mM (Table 1).

Regarding data from NR uptake assay (Table 1), 3,4-DMMC was again the most toxic compound, with LC_{50} values under 2 mM for both tested time-points. On the other hand, with LC_{50} values over 9 mM, *N,N*-dimethylcathinone and *N*-ethylcathinone were the least toxic cathinones after 24 and 48 h incubation, respectively.

It is important to highlight that, with exception of METH, 3,4-DMMC and methcathinone, all tested drugs exhibited a significant increase in cytotoxicity at the later time-point when compared to the 24-h time-point for the MTT assay (Table 1). Also, in the NR assay, more than half of all tested drugs (amfepramone, mephedrone, methcathinone, methedrone, *N,N*-dimethylcathinone, pentedrone, α-PPP and α-PVP) caused a significant increase in cytotoxicity at the 48-h time-point when compared to the earlier time-point, as depicted in Table 1.

3.3. NAC was the most effective protector, partially protecting cells from the toxicity induced by amfepramone, methcathinone, N,N-dimethylcathinone, pentedrone and α-PPP

Since the MTT reduction assay proved generally to be the most sensitive towards the evaluation of cytotoxicity after a 24-h of exposure to the tested compounds, the putative protectors were used against the LC_{50} calculated at 24 h, using that assay.

The protective potential of two antioxidants, 1 mM NAC and 100 μM tiron, the protein synthesis inhibitor, 10 nM CHX, and the DAT inhibitor, 1 μM MPH, was evaluated in the presence of cathinones without the methylenedioxy ring or classical amphetamines. After a pre-treatment with the four different alleged protective compounds, SH-SY5Y cells were co-incubated for 24 h with each synthetic drug. It should be noted that none of that four tested putative protectors alone affected cell viability in this cytotoxicity assay. The obtained data are presented in Fig. 3.

NAC proved to be the most effective protective compound since it partially protected the cells from cytotoxicity induced by AMPH (Fig. 3a), methcathinone (Fig. 3e) and *N,N*-dimethylcathinone (Fig. 3f) while CHX, MPH and tiron had no protective role concerning the toxicity exhibited by the referred drugs (data not shown). Also, NAC was able to prevent the toxicity elicited by amfepramone (Fig. 3c), pentedrone (Fig. 3g) and α-PPP (Fig. 3h). It should be noted that CHX also evidenced a partial protective role against the toxicity evoked by amfepramone (Fig. 3c), while MPH and tiron showed no protection (data not shown). In addition to NAC, both CHX and MPH were able to partially prevent the cytotoxic effect evidenced by pentedrone (Fig. 3g), whilst tiron did not protected the cells incubated with this cathinone (data not shown). α-PPP-induced toxicity was partially prevented not only by NAC, as previously mentioned, but also by MPH and tiron (Fig. 3h), but not by CHX (data not shown).

None of the four putative neuroprotective tested compounds had the ability to counteract the cytotoxicity elicited by METH, flephedrone, mephedrone, methedrone, *N*-ethylcathinone, α-PBP and α-PVP in the MTT reduction assay (data not shown). Surprisingly, pre-treatment with tiron potentiated the cytotoxicity of 3,4-DMMC and buphedrone (Fig. 3b and d, respectively), whilst CHX, MPH and NAC neither

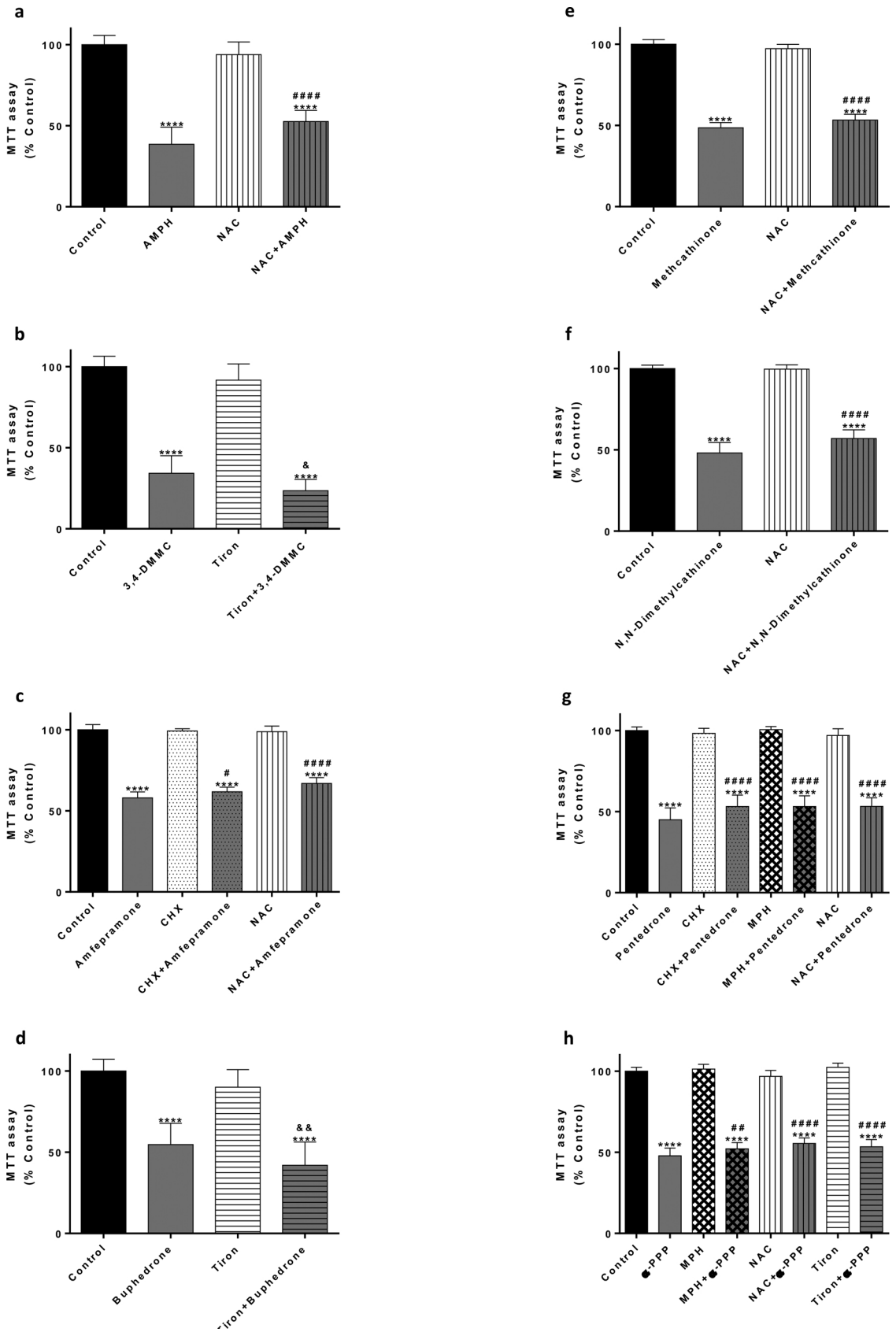

Fig. 3. Evaluation of the protection provided by putative neuroprotectors after exposure to LC_{50} of AMPH or synthetic cathinones. In these experiments, cells underwent a pre-treatment with the putative neuroprotective compounds [10 nM cycloheximide (CHX), 1 μM methylphenidate (MPH), 1 mM *N*-acetyl-L-cysteine (NAC) and 100 μM tiron]. The MTT assay (a, b, c, d, e, f, g and h) was performed 24 h after exposure. Data are presented in percentage of control as mean ± SD. Statistical analyses were performed using one-way ANOVA, followed by the Tukey's post hoc test (from at least 5 independent experiments performed in quadruplicate) [$^{****}p < 0.0001$ all vs. control; $^{\#}p < 0.05$, $^{\#\#}p < 0.01$, $^{\#\#\#\#}p < 0.0001$ neuroprotective compound + LC_{50} vs. LC_{50} (evidence of protection); $^{\&}p < 0.05$, $^{\&\&}p < 0.01$ tiron + LC_{50} vs. LC_{50} (meaning aggravation of cathinone deleterious effect)].

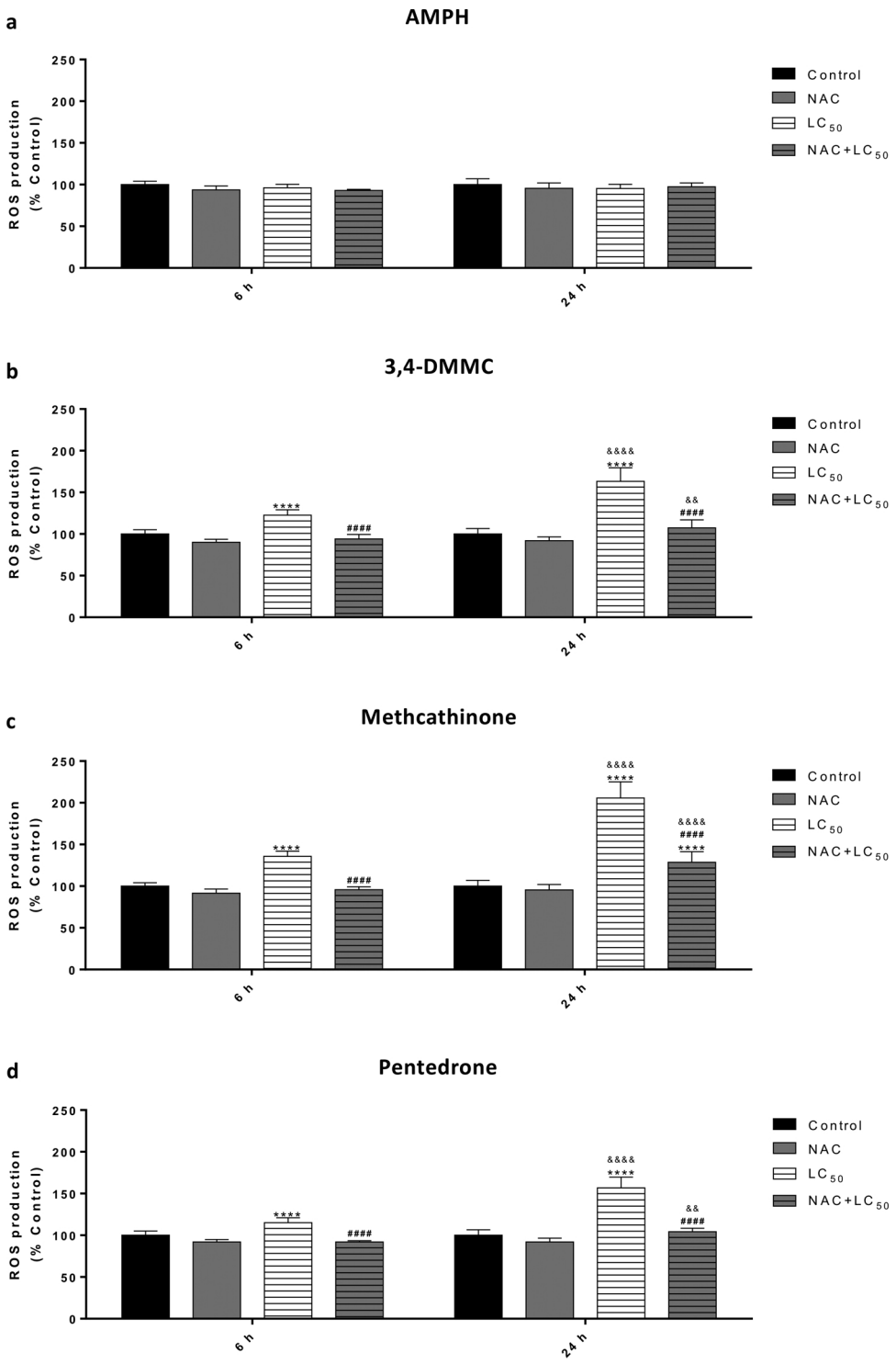

Fig. 4. Assessment of reactive oxygen species (ROS) production, using the 2′,7′-dichlorodihydrofluorescein diacetate probe, on differentiated SH-SY5Y cells exposed for 6- and 24-h to LC_{50} of AMPH (a), 3,4-DMMC (b), methcathinone (c) or pentedrone (d). Also, the putative protection of 30 min pre-incubation of 1 mM *N*-acetyl-L-cysteine (NAC) on ROS production was evaluated. Data are presented in percentage of control as mean ± SD. Statistical analyses were performed using two-way ANOVA with repeated measures, followed by the Sidak's post hoc test (from 3 independent experiments performed in triplicate) [$^{****}p < 0.0001$ all vs. control; $^{####}p < 0.0001$ NAC + LC_{50} vs. LC_{50}; $^{\&\&}p < 0.01$, $^{\&\&\&\&}p < 0.0001$ condition vs. same condition (between different time-points)].

prevented nor exacerbated the cytotoxicity exhibited by the previous two cathinones in this assay (data not shown).

3.4. NAC attenuated the ROS production elicited by 3,4-DMMC, methcathinone and pentedrone

The production of ROS was measured after cells exposure to the LC_{50} of synthetic cathinones (3,4-DMMC, methcathinone and pentedrone) or AMPH, for 6 and 24 h. Additionally, the putative reversal of ROS generation by NAC was also evaluated. Results are displayed in Fig. 4 by alphabetic order, first AMPH followed by the synthetic cathinones.

When compared to control levels, AMPH did not induce a significant production of any ROS (Fig. 4a). On the other hand, the synthetic cathinones herein tested were able to induce a time-dependent increase in ROS production. The increase in ROS was significant at the 6-h time-point for the three cathinones when compared to control cells. Notwithstanding, this effect was far more noticeable at 24 h, as depicted in Fig. 4b–d.

Exposure of cells to NAC, prior to synthetic cathinones incubation, completely inhibited the ROS production exhibited by 3,4-DMMC and pentedrone (Fig. 4b and d, respectively). Despite NAC's remarkable

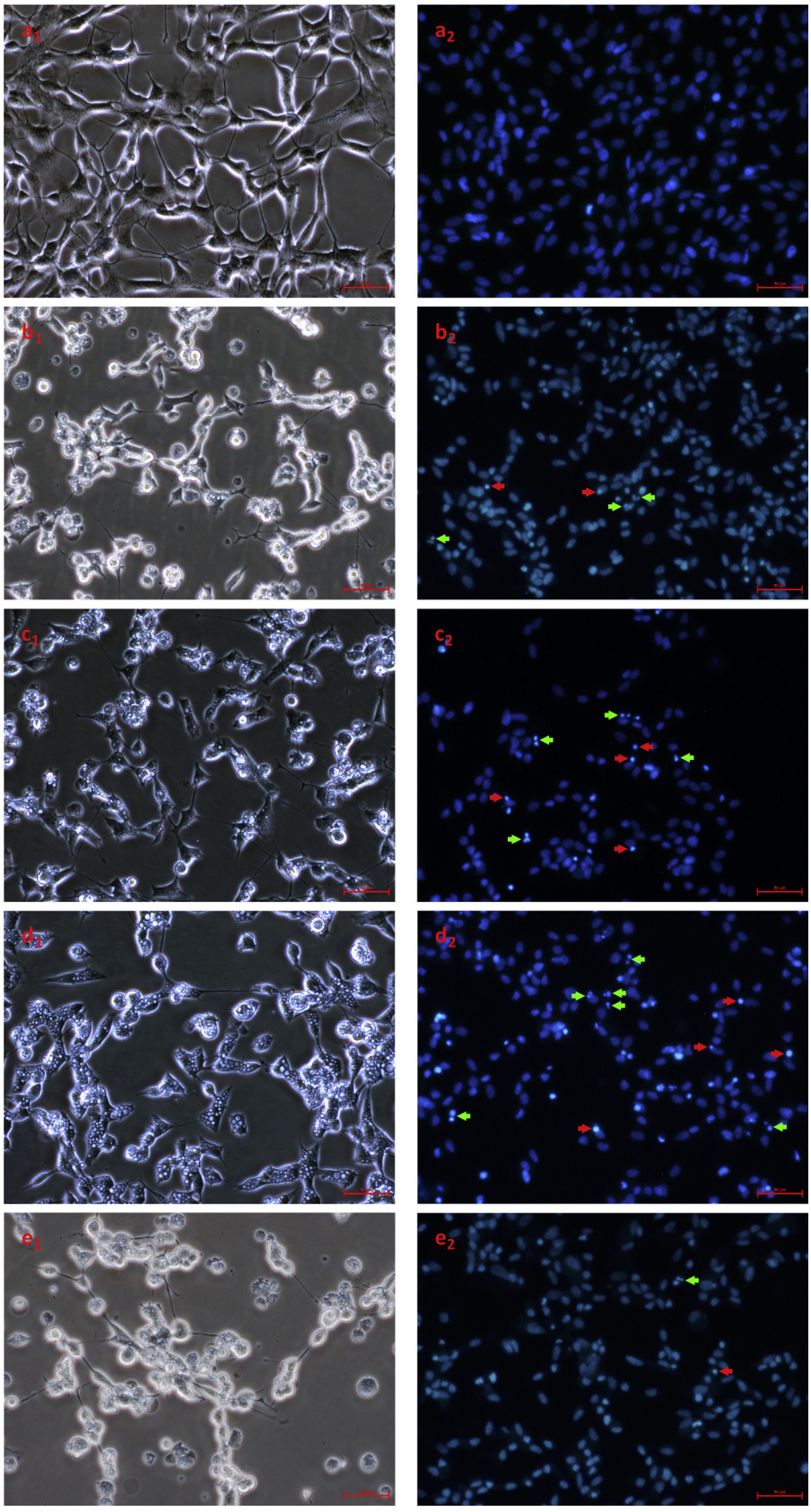

Fig. 5. Morphological analysis of differentiated SH-SY5Y cells exposed for 24 h to LC_{50} of 3,4-DMMC, mephedrone, methcathinone or METH (b_1, c_1, d_1, and e_1, respectively), and the control group (a_1) by phase-contrast microscopy. Microphotographs from Hoechst nuclear staining were taken after a 24-h exposure period to LC_{50} of 3,4-DMMC (b_2), mephedrone (c_2), methcathinone (d_2) or METH (e_2), and comparisons were made to control group (a_2). Inserted green arrows point the pyknotic nuclei, whilst red arrows indicate chromatin condensation. Original magnification x200. Representative microphotographs, from at least three independent experiments, were taken of randomly chosen fields in 48-well plates (scale bar 50 μm) (For interpretation of the references to colour in this figure legend, the reader is referred to the web version of this article).

protective effect observed for 3,4-DMMC and pentedrone, in cells exposed to methcathinone this protective effect was less noticeable (Fig. 4c). It should be noted that NAC alone did not significantly altered ROS levels when compared to control cells.

3.5. 3,4-DMMC, methcathinone, pentedrone and AMPH evoked autophagy activation

We assessed the morphological changes evoked to the cells exposed

for 24 h to the LC_{50} of cathinones without the methylenedioxy ring or classical amphetamines by phase-contrast microscopy and after Hoechst staining (Fig. 5). Morphological changes, such as cytoplasmic shrinkage and neurite retraction were evident in phase-contrast micrographs of cells treated with all synthetic cathinones and amphetamines, which were absent in untreated cells. To illustrate this, we selected 3,4-DMMC, mephedrone, methcathinone and METH, as can be depicted in Fig. 5. Representative micrographs of SH-SY5Y cells exposed to 3,4-DMMC, mephedrone, methcathinone and METH stained with Hoechst 33258 are presented in Fig. 5b_2, c_2, d_2 and e_2, respectively, depicting chromatin condensation (red arrows) and the presence of pyknotic nuclei (green arrows), that were absent in control cells (Fig. 5a_2). Although all the cathinones and classical amphetamines were evaluated by phase-contrast and by Hoechst staining, we have selected the compounds mentioned above as they are representative of all tested compounds.

Interestingly, cells under cathinone exposure displayed notable intracellular vacuolization (Fig. 5b_1, c_1 and d_1), which was not observed in control cells (Fig. 5a_1), suggesting autophagy activation. Drug-induced autophagy was evaluated after exposing cells to the LC_{50} of 3,4-DMMC, methcathinone, pentedrone and AMPH, for 24 h, and incubating them with CYTO-ID® green detection reagent. Also, 3-MA putative protection was assessed by the MTT reduction assay, pre-incubating cells with this autophagy inhibitor prior to the exposure of the cells to the LC_{50} of 3,4-DMMC, methcathinone, pentedrone and AMPH, for 24 h. The obtained results confirmed that both synthetic cathinones and AMPH were able to trigger autophagy, this effect being 1.4–1.5 higher than the positive control chloroquine/rapamycin (Fig. 6a). These results can be confirmed with the representative cytometer event counting in FL1 (Fig. 6b), in which can be depicted that 3,4-DMMC, methcathinone, pentedrone and AMPH peaks are dragged rightwards from the control cells peak, indicating autophagy activation. Although cells exposed to methcathinone had larger rounded vacuoles, it was not the cathinone that induced the highest autophagy activation in the time-point assessed (24 h). As depicted in Fig. 6c, 3-MA was able to reduce the cytotoxicity induced by 3,4-DMMC, pentedrone and AMPH, while having no significant effect regards the protection of cells exposed to methcathinone.

4. Discussion

The present work led to the following major findings: synthetic cathinones lacking the methylenedioxy ring and the classical amphetamines induced a concentration-dependent toxicity in dopaminergic SH-SY5Y cells; fitted concentration-toxicity curves revealed that 3,4-DMMC had the lowest LC_{50} value in both cytotoxicity assays and in the two time-points assessed; synthetic cathinones evoked an increase in ROS production, while NAC totally prevented this last event; synthetic cathinones evoked morphological features of apoptotic death and intracellular vacuolization; 3,4-DMMC, methcathinone and pentedrone triggered autophagy activation.

Synthetic cathinones exhibit strong affinity to DAT, despite differences in binding affinities, and behave as substrates or inhibitors of this monoaminergic transporter (Simmler et al., 2013; Valente et al., 2014). Therefore, dopaminergic SH-SY5Y cells, an *in vitro* model of differentiated neuronal cells, can provide important data regarding the toxicity of cathinones lacking the methylenedioxy ring. We found that although several cathinones had a toxicity profile comparable to that of classical amphetamines, 3,4-DMMC was even more toxic than AMPH and METH. Meanwhile, mephedrone and α-PVP proved to be more toxic than AMPH, though less toxic than METH.

Mitochondrial dysfunction, evaluated by the MTT reduction assay, and NR uptake impairment, which evaluates the lysosomal function, are seen as indirect measures of cytotoxicity (Borenfreund and Puerner, 1985; Mosmann, 1983). Amphetamines and synthetic cathinones were reported to decrease mitochondrial respiration in cultured SH-SY5Y cells (den Hollander et al., 2015), and the MTT reduction assay may be used as a reliable tool for the determination of the cytotoxic profile of synthetic cathinones (Araujo et al., 2015; Valente et al., 2017b). In the present study, all compounds induced cytotoxicity in a concentration-dependent manner, but not all showed time-dependent toxicity, as

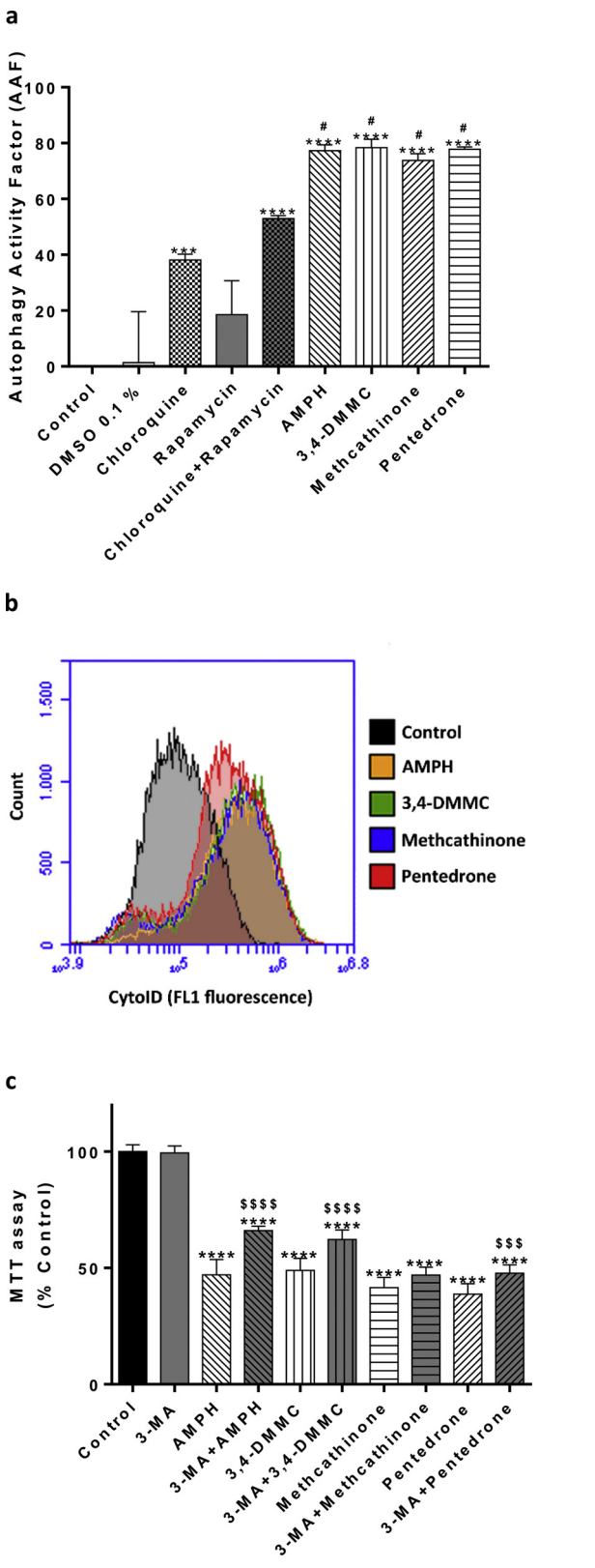

(caption on next page)

Fig. 6. (a) Autophagy activity factor (AAF) values were calculated for differentiated SH-SY5Y cells exposed to LC_{50} of AMPH, 3,4-DMMC, methcathinone or pentedrone, for 24 h. (b) Representative cytometer event counting in FL1 for control cells and LC_{50} of AMPH (placed in yellow), 3,4-DMMC (placed in green), methcathinone (placed in blue) and pentedrone (placed in red). (c) Evaluation of 3-methyladenine (3-MA) putative protection on differentiated SH-SY5Y cells exposed for 24 h to LC_{50} of cathinones or AMPH, assessed through the MTT reduction assay. Data are presented as mean ± SD, from 3 independent experiments (AAF) and 3 independent experiments performed in triplicate (MTT reduction assay). Statistical analyses were performed using one-way ANOVA, followed by the Tukey's post hoc test ($^{***}p < 0.001$, $^{****}p < 0.0001$ all vs. control; $^{\#}p < 0.05$ cathinones or AMPH vs. chloroquine + rapamycin; $^{\$\$\$}p < 0.001$, $^{\$\$\$\$}p < 0.0001$ 3-MA + cathinones or AMPH vs. cathinones or AMPH alone) (For interpretation of the references to colour in this figure legend, the reader is referred to the web version of this article).

observed for METH, 3,4-DMMC and methcathinone, regarding the MTT reduction assay. In agreement with our results, Martinez-Clemente et al. (2014) observed a concentration- and time-dependent toxicity induced by mephedrone in mouse cortical cultured neurons, also by using the MTT reduction assay. In the present study, NR uptake data indicated that cytotoxicity was concentration- and time-dependent for a large number of synthetic cathinones with exception of 3,4-DMMC, buphedrone, flephedrone, *N*-ethylcathinone and *α*-PBP for which no significant increase in cytotoxicity was observed between the two time-points. Importantly, we observed that the MTT reduction assay was overall more sensitive than the NR uptake assay to the toxicity of these drugs. Correlating these results to the obtained LC_{50} values for both cytotoxicity assays, for example for flephedrone and buphedrone, the LC_{50} in the NR uptake assay is about 1.5 and 2 times higher, respectively, than the LC_{50} in the MTT reduction test. This might be due to the fact that in cell culture medium, cathinones, such as mephedrone, can be converted to its methylbenzamide breakdown product, which, by itself, is able to decrease mitochondrial respiration in neuronal cells (den Hollander et al., 2015). To the best of our knowledge, no other study compared the toxicity of such a large number of cathinones in neuronal models.

MTT reduction data allowed us to describe a putative structure-activity relationship regarding the toxicity profile of the studied synthetic cathinones (Fig. 7): the shortening of the lipophilic chain (R_3) decreases the cytotoxicity of the molecule (*α*-PVP > *α*-PBP > α-PPP; pentedrone > buphedrone > methcathinone); the higher steric bulk of R_2 substituent, the greater the molecules' cytotoxicity (mephedrone > methedrone > flephedrone > methcathinone), being methedrone the only exception, that may have to do with the fact that the methoxy group, although more bulky, is further away from the binding site; alkyl substituents on R_1 and R_2 increases the cytotoxicity of the molecule (3,4-DMMC > mephedrone > methedrone > flephedrone > methcathinone); substitution of the pyrrolidine ring (R_4 and R_5) by an acyclic secondary amine moiety resulted in an increase of cytotoxicity (methcathinone > *N*-ethylcathinone > *α*-PPP; buphedrone > *α*-PBP); substitution of the pyrrolidine ring (R_4 and R_5) by a tertiary amine moiety resulted in a decrease of cytotoxicity (*α*-PPP > *N,N*-dimethylcathinone ≈ amfepramone). These findings are in line with other studies showing a reduction in potency of the molecule as reuptake inhibitor at DAT, when a shortening of the lipophilic chain in R_3 occurs (Kolanos et al., 2015; Marusich et al., 2014). Furthermore, other authors affirmed that an increase in *α*-lipophilic chain (R_3) is responsible for an increasing potency as DAT inhibitors of *α*-pyrrolidinophenones (Eshleman et al., 2017). Other authors showed that when neuronal SK-*N*-SH cells are incubated for 48 h with *α*-PVP (range of concentrations 10–50 μM) no significant decrease in cell viability is seen. However, *α*-pyrrolidinononanophenone (*α*-PNP), a synthetic cathinone with a longer lipophilic chain than *α*-PVP, significantly lowered the cells' viability in the same experimental conditions (Matsunaga et al., 2017). Secondly, Negus and Banks (2017) analysis suggested that larger R_2 substituent bulk is correlated with a decrease of potency on monoamine release via DAT. Another study reported mephedrone as being more potent inhibitor of DA uptake at DAT than flephedrone and methcathinone (Eshleman et al., 2013), which agrees with our proposal of a structure-toxicity profile. The replacement of the pyrrolidine ring of methylenedioxypyrovalerone (MDPV) by its tertiary, secondary or primary amine analogues resulted in a progressive and orderly decrease in potency of this synthetic cathinone as a reuptake inhibitor at DAT (Glennon and Young, 2016), which may be partially correlated with our findings. Eshleman et al. (2017) data corroborate our findings presenting *α*-PPP as less potent than methcathinone in monoamine uptake at DAT. To the best of our knowledge, there are no other published studies of structure-activity relationship regarding the toxicity profile of these thirteen studied cathinones.

It is known that classical amphetamines, once inside the neuron, cause the disruption of neurotransmitter vesicular storage increasing the cytosol levels of DA (Teixeira-Gomes et al., 2015). The rising of intracellular DA levels increases its predisposal for oxidation and metabolism, leading to the formation of ROS, which have a conspicuous role on the cytotoxicity exerted by classical amphetamines (Angoa-Perez et al., 2017). The structural similarity of synthetic cathinones with classical amphetamines led us to believe that cathinones toxicity could be prevented by antioxidant molecules, such as NAC, a potent antioxidant agent, used for its properties as ROS scavenger and a glutathione precursor (Capela et al., 2006Ferreira et al., 2013), or tiron, which easily enters the cells and scavenge superoxide anion radical and free electrons (Taiwo, 2008). Herein, NAC showed to be the most effective neuroprotective compound as it prevented the toxicity of several cathinones, which may suggest an important role for oxidative stress in the cytotoxicity induced not only by classical amphetamines but also by synthetic cathinones. Accordingly, on recent studies from our group, NAC protected differentiated SH-SY5Y cells against the toxicity exerted by AMPH for 24 h, both on the MTT reduction and the lactate dehydrogenase leakage assays (Feio-Azevedo et al., 2017), while fully reverting ROS production after 24 h of exposure to methylone or MDPV (Valente et al., 2017a). These data support the involvement of oxidative stress on AMPH- and cathinones-induced toxicity. In the present study, tiron partially protected cells against the toxicity induced by *α*-PPP, indicating that the increase in superoxide anion radical may be partially responsible for its toxicity mechanisms. Few studies had demonstrated the neuroprotective potential of this antioxidant. In fact, our group has shown that tiron had no effect on the neurotoxicity induced by ecstasy or its metabolites in the same *in vitro* model (Ferreira et al., 2013). On the other hand, Lukandu et al. (2008) showed that tiron was more effective than NAC regarding the protection of keratinocytes and fibroblasts from khat-induced cytotoxicity. Interestingly, in the present study, this antioxidant further heightened 3,4-DMMC- and buphedrone-induced toxicity. Although NAC and tiron both have antioxidant properties, the major difference concerned to their action mechanisms can be mainly related with the fact that NAC is also a cysteine donor used in glutathione production, and not only a broad scavenger of ROS.

Pre-treatment with CHX, a protein synthesis inhibitor, induces the formation of neuroprotective gene products, as anti-apoptotic gene *Bcl-2* and antioxidant enzymes (Furukawa et al., 1997). A study showed that cell death induced by a khat extract (200 μg mL^{-1}) was inhibited when HL-60 cells were pre-incubated with low to moderate CHX concentrations (31.6–100 ng mL^{-1}) (Dimba et al., 2004). In our study, CHX partially prevented the cytotoxicity induced by amfepramone and pentedrone. Of note, these are the only cathinones that elicited greater lysosomal dysfunction than mitochondrial impairment at the 24-h time-point (Table 1). In addition, cells exposed to these two cathinones displayed vesicular organelles in phase-contrast microphotographs, but lower than those produced by other cathinones, namely methcathinone. Thus, we can speculate that pre-treatment with CHX could lead to protein synthesis inhibition that would be crucial to the authopagic

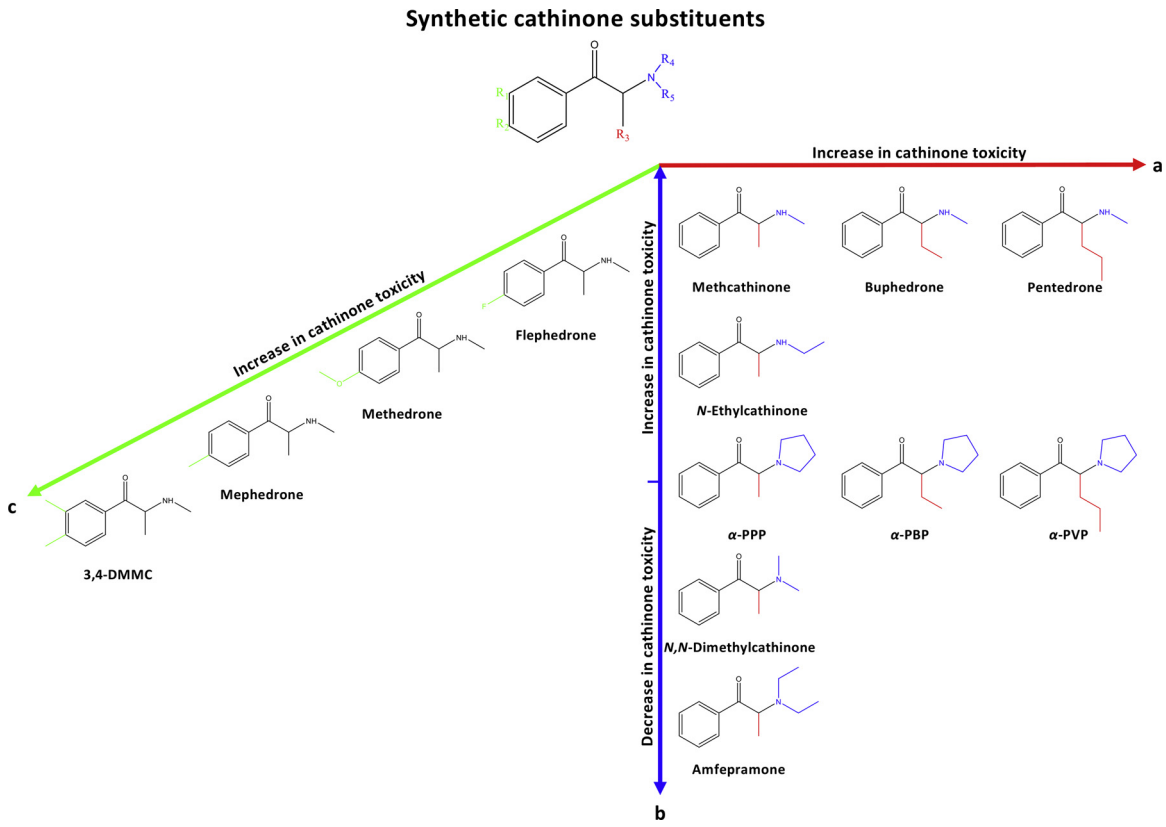

Fig. 7. General relationship of the structure of synthetic cathinones and their dopaminergic toxicity, considering the MTT reduction assay LC_{50} values for the 24-h time-point. Cathinones core chemical structure is presented in black. R_1 and R_2 (displayed in green), R_3 (displayed in red), R_4 and R_5 (displayed in blue) are possible sites where different substituents can be attached. The different colours are related to the three different axes. Axis a is displayed in red and represents the increase in cathinone toxicity with the α-lipophilic chain elongation. Axis b (displayed in blue) regards the substitution of pyrrolidine ring by a secondary or tertiary acyclic amine, which characterises an increase or decrease, respectively, in toxicity of these compounds. Axis c, (displayed in green) in which can be depicted the increased toxicity of substituted cathinones, is related to the substitutions on the aromatic ring. It should be noted, that pentedrone is less toxic than *α*-PVP, representing the only exception in this schematic structure-activity relationship, regarding cathinones toxicity (For interpretation of the references to colour in this figure legend, the reader is referred to the web version of this article).

vesicles development in cells exposed to those cathinones.

It has been suggested that the entry of synthetic cathinones, as mephedrone, occurs via DAT (den Hollander et al., 2015). We showed that MPH partially protected cells from cytotoxicity induced by pentedrone and *α*-PPP in the MTT reduction assay. Feio-Azevedo et al. (2017) showed, using the LDH release assay, that MPH partially protected SH-SY5Y cells exposed to 3.5 mM AMPH for 24 h, highlighting the importance of this entrance route to AMPH-related toxicity. In agreement, GBR 12909 (other selective DAT blocker) protected SH-SY5Y cells exposed to 2 mM mephedrone for 48 h (den Hollander et al., 2015). Some authors showed that the MPH concentration required to inhibit DAT was circa 0.1 μM (Eshleman et al., 1999; Han and Gu, 2006), while the use of MPH at higher concentrations (5000 ng/mL, about 18 μM) led to a significant reduction in SH-SY5Y cell viability (Schmidt et al., 2010). Thus, 1 μM MPH appears to be an appropriate concentration for DAT blocking without having any negative effect on cell viability. Even so, we did not observe a significant protection when using MPH, therefore the concentration used in the present study might not be sufficient to fully inhibit DAT since we tested this DAT blocker, at micromolar range, against a millimolar concentration range of synthetic cathinones. Notwithstanding, cathinones may also enter the neurons via simple diffusion, as shown for AMPH and mephedrone (den Hollander et al., 2015; Teixeira-Gomes et al., 2015), and future studies of kinetic experiments with extracellular dopamine and synthetic cathinones labelled with epitopes must be done to clarify their entrance in neurons.

Few studies have addressed the synthetic cathinones without the methylenedioxy ring-induced apoptosis in neuronal models. It is known that classical amphetamines lead to neuronal cell death by apoptosis (Angoa-Perez et al., 2017). In our work, all tested compounds induced apoptotic features in SH-SY5Y differentiated cells, including pyknotic nuclei on Hoechst nuclear staining, while the control cells exhibited a fusiform shape, undamaged cytoplasmic membrane, well-formed dendrites and good adherence. Several studies show that amphetamines induce neuronal apoptosis both in humans and in animal models. For instance, ecstasy induced apoptosis in cultured rat cortical neurons after a 48-h of exposure to the drug (100–800 μM) (Capela et al., 2007a). On another study, cerebellar granule neurons underwent apoptosis after treatment with METH or ecstasy (1–5 mM) for 24 h or 48 h (Jimenez et al., 2004). Moreover, other authors have shown that exposure for 96 h to 500 μM D-AMPH, METH, methylenedioxyamphetamine or ecstasy induced apoptosis in cultured rat neocortical neurons (Stumm et al., 1999). Differentiated SH-SY5Y cells undergo apoptosis when exposed to the effective concentration 30 % (1.962 mM and 1.165 mM, respectively) and to the effective concentration 60 % (2.797 mM and 1.703 mM, respectively) of two synthetic cathinones with the methylenedioxy ring (methylone and MDPV) for 24 h (Valente et al., 2017b). Others have reported that human neuronal SK-*N*-SH cells exposed for 48 h to *α*-PNP (50 μM) also undergo apoptosis (Matsunaga et al., 2017). Siedlecka-Kroplewska et al. (2018) demonstrated that 3-fluoromethcathinone induced a remarkable apoptotic cell death in neuronal HT22 cells after exposure to 4 mM of this cathinone for a 24-h period. Moreover, an intraperitoneal injection of 10 mg/Kg MDPV specially increases the apoptotic death of neurons from nucleus

accumbens of 7-day-old post-embryonic mice (Adam et al., 2014). Taken together, our results further support an important role of apoptosis in the cytotoxicity of synthetic cathinones.

In addition to apoptosis, amphetamines are also capable of inducing the activation of autophagic mechanisms (Chandramani Shivalingappa et al., 2012; Li et al., 2014). Recent studies have demonstrated the activation of autophagy in different neuronal cell models when exposed to cathinones without the methylenedioxy ring (Matsunaga et al., 2017; Siedlecka-Kroplewska et al., 2018), or with the methylenedioxy ring (Valente et al., 2017a). Our phase-contrast micrographs clearly show the presence of vesicular organelles in cells exposed to the cathinones. Moreover, we found that synthetic cathinones, as 3,4-DMMC, methcathinone and pentedrone, and also AMPH triggered autophagy activation in differentiated SH-SY5Y cells. Furthermore, it has been demonstrated that amphetamines and synthetic cathinones induce both oxidative stress and autophagy (Kanthasamy et al., 2006; Matsunaga et al., 2017; Siedlecka-Kroplewska et al., 2018; Valente et al., 2017a). In fact, as a consequence of oxidative stress, a dysregulation in cell homeostasis can occur, with accumulation of damaged proteins and/or organelles. In the present study, 3,4-DMMC, methcathinone and pentedrone induced oxidative stress by increasing significantly ROS production. 3-MA provided partial protection against 3,4-DMMC- and pentedrone-induced cytotoxicity, possibly activated by the redox status imbalance elicited by these substances. As AMPH-induced cytotoxicity was also prevented by 3-MA, autophagy activation might be triggered, leading to cell death. However, the autophagy pathways triggered in cathinones-induced neurotoxicity remain unclear, and more studies are needed.

The millimolar range of concentrations used herein is mainly interesting from a structure-activity point of view. We investigated the cytotoxicity of synthetic cathinones in a neuronal model using the millimolar range to obtain concentration-toxicity curves and rank compounds in terms of toxic potential. The lowest LC_{50} of 1.2 mM was obtained for 3,4-DMMC, which is several fold above the reported affinity of these compounds to DAT (in the nM or low μM range) or DA receptor (in the μM range) (Baumann et al., 2012; Hondebrink et al., 2018; Kolanos et al., 2015; Marusich et al., 2014; Zwartsen et al., 2017). Nevertheless, our study reveals a structure-toxicity profile that can steer future research to more sensitive endpoints, possibly more relevant to the human exposure scenario.

5. Conclusion

In conclusion, this was the first study to comparatively evaluate the cytotoxicity of such a broad range of cathinones without the methylenedioxy ring. We were able to establish a structure-toxicity profile for these compounds, which evoked autophagy, increased ROS production and presented apoptotic features of cell death. Moreover, in the used *in vitro* model, 3,4-DMMC was more toxic than classical amphetamines. Meanwhile, mephedrone, *α*-PVP and methedrone cytotoxicity was comparable to that of the tested classical amphetamines. More studies are needed to disclose the underlying mechanisms of neurotoxicity of these new psychoactive substances, besides oxidative stress or autophagy, since other mechanisms seemed to be involved.

Transparency document

The Transparency document associated with this article can be found in the online version.

Declaration of Competing Interest

The authors declare that there is no conflict of interest.

Acknowledgments

Jorge Soares acknowledges University of Porto/Faculty of Medicine University of Porto through FSE - Fundo Social Europeu, NORTE2020 - Programa Operacional Regional do Norte for his grant (NORTE-08-5369-FSE-000011). This work received financial support from the European Union (FEDER funds POCI/01/0145/FEDER/007728) and National Funds (FCT/MEC, Fundação para a Ciência e a Tecnologia and Ministério da Educação e Ciência) under the Partnership Agreement PT2020 UID/MULTI/04378/2013 (UCIBIO), UID/MULTI/00612/2013 (CQB), UID/MAR/04292/2013 (MARE) and UID/Multi/04046/2013 (BioISI). Also supported by the project NORTE-01-0145-FEDER-000024, supported by Norte Portugal Regional Operational Programme (NORTE 2020), under the PORTUGAL 2020 Partnership Agreement (DESignBIOtecHealth—New Technologies for three Health Challenges of Modern Societies: Diabetes, Drug Abuse and Kidney Diseases), through the European Regional Development Fund (ERDF). Vera Marisa Costa acknowledges Fundação da Ciência e Tecnologia (FCT) for her grant (SFRH/BPD/110001/2015). The authors wish to thank the Laboratório de Polícia Científica da Polícia Judiciária (LPC-PJ) for providing the smartshop products within the scope of the protocol established between LPC-PJ, FCUL and FFUP.

Appendix A. Supplementary data

Supplementary material related to this article can be found, in the online version, at doi:https://doi.org/10.1016/j.neuro.2019.08.009.

References

Adam, A., Gerecsei, L.I., Lepesi, N., Csillag, A., 2014. Apoptotic effects of the' designer drug' methylenedioxypyrovalerone (MDPV) on the neonatal mouse brain. Neurotoxicology 44, 231–236.
Albertson, T.E., 2014. Recreational drugs of abuse. Clin. Rev. Allergy Immunol. 46 (1), 1–2.
Alotaibi, M.R., Husbands, S.M., Blagbrough, I.S., 2015. (1)H, (1)(3)C, (1)(5)N HMBC, and (1)(9)F NMR spectroscopic characterisation of seized flephedrone, cut with benzocaine. J. Pharm. Biomed. Anal. 107, 535–538.
Angoa-Perez, M., Anneken, J.H., Kuhn, D.M., 2017. Neurotoxicology of synthetic cathinone analogs. Curr. Top. Behav. Neurosci. 32, 209–230.
Araujo, A.M., Valente, M.J., Carvalho, M., Dias da Silva, D., Gaspar, H., Carvalho, F., Bastos, M.L., Guedes de Pinho, P., 2015. Raising awareness of new psychoactive substances: chemical analysis and in vitro toxicity screening of' legal high' packages containing synthetic cathinones. Arch. Toxicol. 89 (5), 757–771.
Archer, R.P., 2009. Fluoromethcathinone, a new substance of abuse. Forensic Sci. Int. 185 (1-3), 10–20.
Barbosa, D.J., Capela, J.P., Silva, R., Vilas-Boas, V., Ferreira, L.M., Branco, P.S., Fernandes, E., Bastos, M.L., Carvalho, F., 2014. The mixture of "ecstasy" and its metabolites is toxic to human SH-SY5Y differentiated cells at in vivo relevant concentrations. Arch. Toxicol. 88 (2), 455–473.
Baumann, M.H., Ayestas Jr., M.A., Partilla, J.S., Sink, J.R., Shulgin, A.T., Daley, P.F., Brandt, S.D., Rothman, R.B., Ruoho, A.E., Cozzi, N.V., 2012. The designer methcathinone analogs, mephedrone and methylone, are substrates for monoamine transporters in brain tissue. Neuropsychopharmacology 37 (5), 1192–1203.
Borenfreund, E., Puerner, J.A., 1985. A simple quantitative procedure using monolayer culture for toxicity assays. J. Tissue Cult. Methods 9 (1), 7–9.
Boulanger-Gobeil, C., St-Onge, M., Laliberte, M., Auger, P.L., 2012. Seizures and hyponatremia related to ethcathinone and methylone poisoning. J. Med. Toxicol. 8 (1), 59–61.
Capela, J.P., Fernandes, E., Remiao, F., Bastos, M.L., Meisel, A., Carvalho, F., 2007a. Ecstasy induces apoptosis via 5-HT(2A)-receptor stimulation in cortical neurons. Neurotoxicology 28 (4), 868–875.
Capela, J.P., Macedo, C., Branco, P.S., Ferreira, L.M., Lobo, A.M., Fernandes, E., Remiao, F., Bastos, M.L., Dirnagl, U., Meisel, A., Carvalho, F., 2007b. Neurotoxicity mechanisms of thioether ecstasy metabolites. Neuroscience 146 (4), 1743–1757.
Capela, J.P., Meisel, A., Abreu, A.R., Branco, P.S., Ferreira, L.M., Lobo, A.M., Remiao, F., Bastos, M.L., Carvalho, F., 2006. Neurotoxicity of Ecstasy metabolites in rat cortical neurons, and influence of hyperthermia. J. Pharmacol. Exp. Ther. 316 (1), 53–61.
Chan, L.L., Shen, D., Wilkinson, A.R., Patton, W., Lai, N., Chan, E., Kuksin, D., Lin, B., Qiu, J., 2012. A novel image-based cytometry method for autophagy detection in living cells. Autophagy 8 (9), 1371–1382.
Chandramani Shivalingappa, P., Jin, H., Anantharam, V., Kanthasamy, A., Kanthasamy, A., 2012. N-acetyl cysteine protects against methamphetamine-induced dopaminergic neurodegeneration via modulation of redox status and autophagy in dopaminergic cells. Parkinsons Dis. 2012, 424285.
Costa, V.M., Silva, R., Tavares, L.C., Vitorino, R., Amado, F., Carvalho, F., Bastos, M.L.,

Carvalho, M., Carvalho, R.A., Remiao, F., 2009. Adrenaline and reactive oxygen species elicit proteome and energetic metabolism modifications in freshly isolated rat cardiomyocytes. Toxicology 260 (1-3), 84–96.
den Hollander, B., Sundstrom, M., Pelander, A., Siltanen, A., Ojanpera, I., Mervaala, E., Korpi, E.R., Kankuri, E., 2015. Mitochondrial respiratory dysfunction due to the conversion of substituted cathinones to methylbenzamides in SH-SY5Y cells. Sci. Rep. 5, 14924.
Dimba, E.A., Gjertsen, B.T., Bredholt, T., Fossan, K.O., Costea, D.E., Francis, G.W., Johannessen, A.C., Vintermyr, O.K., 2004. Khat (Catha edulis)-induced apoptosis is inhibited by antagonists of caspase-1 and -8 in human leukaemia cells. Br. J. Cancer 91 (9), 1726–1734.
Dolengevich-Segal, H., Rodriguez-Salgado, B., Gomez-Arnau, J., Sanchez-Mateos, D., 2016. Severe psychosis, drug dependence, and hepatitis C related to slamming mephedrone. Case Rep. Psychiatry 2016, 8379562.
EMCDDA, 2018. European Drug Report 2018: Trends and Developments. Publications Office of the European Union, Luxembourg.
Eshleman, A.J., Carmolli, M., Cumbay, M., Martens, C.R., Neve, K.A., Janowsky, A., 1999. Characteristics of drug interactions with recombinant biogenic amine transporters expressed in the same cell type. J. Pharmacol. Exp. Ther. 289 (2), 877–885.
Eshleman, A.J., Wolfrum, K.M., Hatfield, M.G., Johnson, R.A., Murphy, K.V., Janowsky, A., 2013. Substituted methcathinones differ in transporter and receptor interactions. Biochem. Pharmacol. 85 (12), 1803–1815.
Eshleman, A.J., Wolfrum, K.M., Reed, J.F., Kim, S.O., Swanson, T., Johnson, R.A., Janowsky, A., 2017. Structure-activity relationships of substituted cathinones, with transporter binding, uptake, and release. J. Pharmacol. Exp. Ther. 360 (1), 33–47.
Feio-Azevedo, R., Costa, V.M., Ferreira, L.M., Branco, P.S., Pereira, F.C., Bastos, M.L., Carvalho, F., Capela, J.P., 2017. Toxicity of the amphetamine metabolites 4-hydroxyamphetamine and 4-hydroxynorephedrine in human dopaminergic differentiated SH-SY5Y cells. Toxicol. Lett. 269, 65–76.
Ferreira, P.S., Nogueira, T.B., Costa, V.M., Branco, P.S., Ferreira, L.M., Fernandes, E., Bastos, M.L., Meisel, A., Carvalho, F., Capela, J.P., 2013. Neurotoxicity of "ecstasy" and its metabolites in human dopaminergic differentiated SH-SY5Y cells. Toxicol. Lett. 216 (2-3), 159–170.
Furukawa, K., Estus, S., Fu, W., Mark, R.J., Mattson, M.P., 1997. Neuroprotective action of cycloheximide involves induction of bcl-2 and antioxidant pathways. J. Cell Biol. 136 (5), 1137–1149.
Gaspar, H., Bronze, S., Ciriaco, S., Queiros, C.R., Matias, A., Rodrigues, J., Oliveira, C., Cordeiro, C., Santos, S., 2015. 4F-PBP (4′-fluoro-alpha-pyrrolidinobutyrophenone), a new substance of abuse: Structural characterization and purity NMR profiling. Forensic Sci. Int. 252, 168–176.
Gaspar, H., Bronze, S., Oliveira, C., Victor, B.L., Machuqueiro, M., Pacheco, R., Caldeira, M.J., Santos, S., 2018. Proactive response to tackle the threat of emerging drugs: synthesis and toxicity evaluation of new cathinones. Forensic Sci. Int. 290, 146–156.
German, C.L., Fleckenstein, A.E., Hanson, G.R., 2014. Bath salts and synthetic cathinones: an emerging designer drug phenomenon. Life Sci. 97 (1), 2–8.
Glennon, R.A., Young, R., 2016. Neurobiology of 3,4-methylenedioxypyrovalerone (MDPV) and alpha-pyrrolidinovalerophenone (alpha-PVP). Brain Res. Bull. 126 (Pt 1), 111–126.
Gunderson, E.W., Kirkpatrick, M.G., Willing, L.M., Holstege, C.P., 2013. Substituted cathinone products: a new trend in "bath salts" and other designer stimulant drug use. J. Addict. Med. 7 (3), 153–162.
Han, D.D., Gu, H.H., 2006. Comparison of the monoamine transporters from human and mouse in their sensitivities to psychostimulant drugs. BMC Pharmacol. 6 (6).
Hondebrink, L., Zwartsen, A., Westerink, R.H.S., 2018. Effect fingerprinting of new psychoactive substances (NPS): what can we learn from in vitro data? Pharmacol. Ther. 182, 193–224.
Jimenez, A., Jorda, E.G., Verdaguer, E., Pubill, D., Sureda, F.X., Canudas, A.M., Escubedo, E., Camarasa, J., Camins, A., Pallas, M., 2004. Neurotoxicity of amphetamine derivatives is mediated by caspase pathway activation in rat cerebellar granule cells. Toxicol. Appl. Pharmacol. 196 (2), 223–234.
Kanthasamy, A., Anantharam, V., Ali, S.F., Kanthasamy, A.G., 2006. Methamphetamine induces autophagy and apoptosis in a mesencephalic dopaminergic neuronal culture model: role of cathepsin-D in methamphetamine-induced apoptotic cell death. Ann. N. Y. Acad. Sci. 1074, 234–244.
Katz, D.P., Bhattacharya, D., Bhattacharya, S., Deruiter, J., Clark, C.R., Suppiramaniam, V., Dhanasekaran, M., 2014. Synthetic cathinones: "a khat and mouse game". Toxicol. Lett. 229 (2), 349–356.
Kelly, J.P., 2011. Cathinone derivatives: a review of their chemistry, pharmacology and toxicology. Drug Test. Anal. 3 (7-8), 439–453.
Kolanos, R., Sakloth, F., Jain, A.D., Partilla, J.S., Baumann, M.H., Glennon, R.A., 2015. Structural Modification of the Designer Stimulant alpha-Pyrrolidinovalerophenone (alpha-PVP) Influences Potency at Dopamine Transporters. ACS Chem. Neurosci. 6 (10), 1726–1731.
Li, I.H., Ma, K.H., Weng, S.J., Huang, S.S., Liang, C.M., Huang, Y.S., 2014. Autophagy activation is involved in 3,4-methylenedioxymethamphetamine ('ecstasy')-induced neurotoxicity in cultured cortical neurons. PLoS One 9 (12), e116565.
Lopez-Arnau, R., Martinez-Clemente, J., Rodrigo, T., Pubill, D., Camarasa, J., Escubedo, E., 2015. Neuronal changes and oxidative stress in adolescent rats after repeated exposure to mephedrone. Toxicol. Appl. Pharmacol. 286 (1), 27–35.
Ludolph, A.G., Schaz, U., Storch, A., Liebau, S., Fegert, J.M., Boeckers, T.M., 2006. Methylphenidate exerts no neurotoxic, but neuroprotective effects in vitro. J. Neural Transm. Vienna (Vienna) 113 (12), 1927–1934.
Lukandu, O.M., Costea, D.E., Neppelberg, E., Johannessen, A.C., Vintermyr, O.K., 2008. Khat (Catha edulis) induces reactive oxygen species and apoptosis in normal human oral keratinocytes and fibroblasts. Toxicol. Sci. 103 (2), 311–324.
Marinetti, L.J., Antonides, H.M., 2013. Analysis of synthetic cathinones commonly found in bath salts in human performance and postmortem toxicology: method development, drug distribution and interpretation of results. J. Anal. Toxicol. 37 (3), 135–146.
Martinez-Clemente, J., Lopez-Arnau, R., Abad, S., Pubill, D., Escubedo, E., Camarasa, J., 2014. Dose and time-dependent selective neurotoxicity induced by mephedrone in mice. PLoS One 9 (6), e99002.
Martins, J.B., Bastos, M.L., Carvalho, F., Capela, J.P., 2013. Differential effects of Methyl-4-Phenylpyridinium ion, rotenone, and paraquat on differentiated SH-SY5Y cells. J. Toxicol. 2013, 347312.
Marusich, J.A., Antonazzo, K.R., Wiley, J.L., Blough, B.E., Partilla, J.S., Baumann, M.H., 2014. Pharmacology of novel synthetic stimulants structurally related to the "bath salts" constituent 3,4-methylenedioxypyrovalerone (MDPV). Neuropharmacology 87, 206–213.
Mas-Morey, P., Visser, M.H., Winkelmolen, L., Touw, D.J., 2013. Clinical toxicology and management of intoxications with synthetic cathinones ("bath salts"). J. Pharm. Pract. 26 (4), 353–357.
Matsunaga, T., Morikawa, Y., Kamata, K., Shibata, A., Miyazono, H., Sasajima, Y., Suenami, K., Sato, K., Takekoshi, Y., Endo, S., El-Kabbani, O., Ikari, A., 2017. Alpha-Pyrrolidinononanophenone provokes apoptosis of neuronal cells through alterations in antioxidant properties. Toxicology 386, 93–102.
McDermott, S.D., Power, J.D., Kavanagh, P., O'Brien, J., 2011. The analysis of substituted cathinones. Part 2: an investigation into the phenylacetone based isomers of 4-methylmethcathinone and N-ethylcathinone. Forensic Sci. Int. 212 (1-3), 13–21.
Mosmann, T., 1983. Rapid colorimetric assay for cellular growth and survival: application to proliferation and cytotoxicity assays. J. Immunol. Methods 65 (1-2), 55–63.
Negus, S.S., Banks, M.L., 2017. Decoding the structure of abuse potential for new psychoactive substances: structure-activity relationships for abuse-related effects of 4-Substituted methcathinone analogs. Curr. Top. Behav. Neurosci. 32, 119–131.
Nic Daeid, N., Savage, K.A., Ramsay, D., Holland, C., Sutcliffe, O.B., 2014. Development of gas chromatography-mass spectrometry (GC-MS) and other rapid screening methods for the analysis of 16′legal high' cathinone derivatives. Sci. Justice 54 (1), 22–31.
Olives, T.D., Orozco, B.S., Stellpflug, S.J., 2012. Bath salts: the ivory wave of trouble. West. J. Emerg. Med. 13 (1), 58–62.
Prokhorova, E.A., Zamaraev, A.V., Kopeina, G.S., Zhivotovsky, B., Lavrik, I.N., 2015. Role of the nucleus in apoptosis: signaling and execution. Cell. Mol. Life Sci. 72 (23), 4593–4612.
Prosser, J.M., Nelson, L.S., 2012. The toxicology of bath salts: a review of synthetic cathinones. J. Med. Toxicol. 8 (1), 33–42.
Reis-Mendes, A., Gomes, A.S., Carvalho, R.A., Carvalho, F., Remiao, F., Pinto, M., Bastos, M.L., Sousa, E., Costa, V.M., 2017. Naphthoquinoxaline metabolite of mitoxantrone is less cardiotoxic than the parent compound and it can be a more cardiosafe drug in anticancer therapy. Arch. Toxicol. 91 (4), 1871–1890.
Rojek, S., Kula, K., Maciow-Glab, M., Klys, M., 2016. New psychoactive substance alpha-PVP in a traffic accident case. Forensic Toxicol. 34, 403–410.
Schmidt, A.J., Krieg, J.C., Clement, H.W., Gebhardt, S., Schulz, E., Heiser, P., 2010. Impact of drugs approved for treating ADHD on the cell survival and energy metabolism: an in-vitro study in human neuronal and immune cells. J. Psychopharmacol. (Oxford) 24 (12), 1829–1833.
Siedlecka-Kroplewska, K., Wronska, A., Stasilojc, G., Kmiec, Z., 2018. The designer drug 3-Fluoromethcathinone induces oxidative stress and activates autophagy in HT22 neuronal cells. Neurotox. Res. 34 (3), 388–400.
Simmler, L.D., Buser, T.A., Donzelli, M., Schramm, Y., Dieu, L.H., Huwyler, J., Chaboz, S., Hoener, M.C., Liechti, M.E., 2013. Pharmacological characterization of designer cathinones in vitro. Br. J. Pharmacol. 168 (2), 458–470.
Stiles, B.M., Fish, A.F., Cook, C.A., Silva, V., 2016. Bath salt-induced psychosis: nursing assessment, diagnosis, treatment, and outcomes. Perspect. Psychiatr. Care 52 (1), 68–78.
Stumm, G., Schlegel, J., Schafer, T., Wurz, C., Mennel, H.D., Krieg, J.C., Vedder, H., 1999. Amphetamines induce apoptosis and regulation of bcl-x splice variants in neocortical neurons. FASEB J. 13 (9), 1065–1072.
Taiwo, F.A., 2008. Mechanism of tiron as scavenger of superoxide ions and free electrons. Spectroscopy 22, 491–498.
Teixeira-Gomes, A., Costa, V.M., Feio-Azevedo, R., Bastos, M.L., Carvalho, F., Capela, J.P., 2015. The neurotoxicity of amphetamines during the adolescent period. Int. J. Dev. Neurosci. 41, 44–62.
Thornton, M.D., Baum, C.R., 2014. Bath salts and other emerging toxins. Pediatr. Emerg. Care 30 (1), 47–52 quiz 53-45.
Thornton, S.L., Gerona, R.R., Tomaszewski, C.A., 2012. Psychosis from a bath salt product containing flephedrone and MDPV with serum, urine, and product quantification. J. Med. Toxicol. 8 (3), 310–313.
Valente, M.J., Amaral, C., Correia-da-Silva, G., Duarte, J.A., Bastos, M.L., Carvalho, F., Guedes de Pinho, P., Carvalho, M., 2017a. Methylone and MDPV activate autophagy in human dopaminergic SH-SY5Y cells: a new insight into the context of beta-keto amphetamines-related neurotoxicity. Arch. Toxicol. 91 (11), 3663–3676.
Valente, M.J., Araujo, A.M., Bastos, M.L., Fernandes, E., Carvalho, F., Guedes de Pinho, P., Carvalho, M., 2016. Editor's highlight: characterization of hepatotoxicity mechanisms triggered by designer cathinone drugs (beta-Keto amphetamines). Toxicol. Sci. 153 (1), 89–102.
Valente, M.J., Bastos, M.L., Fernandes, E., Carvalho, F., Guedes de Pinho, P., Carvalho, M., 2017b. Neurotoxicity of beta-keto amphetamines: deathly mechanisms elicited by Methylone and MDPV in human dopaminergic SH-SY5Y cells. ACS Chem. Neurosci. 8 (4), 850–859.
Valente, M.J., Guedes de Pinho, P., Bastos, M.L., Carvalho, F., Carvalho, M., 2014. Khat and synthetic cathinones: a review. Arch. Toxicol. 88 (1), 15–45.
Watterson, L.R., Olive, M.F., 2014. Synthetic cathinones and their rewarding and

reinforcing effects in rodents. Adv. Neurosci. (Hindawi) 2014, 209875.
Weaver, M.F., Hopper, J.A., Gunderson, E.W., 2015. Designer drugs 2015: assessment and management. Addict. Sci. Clin. Pract. 10, 8.
Wood, D.M., Dargan, P.I., 2012. Mephedrone (4-methylmethcathinone): what is new in our understanding of its use and toxicity. Prog. Neuropsychopharmacol. Biol. Psychiatry 39 (2), 227–233.
Zhang, B., Cui, Y., Wang, L., Zhao, L., Hou, C., Zeng, Q., Zhang, Z., Yu, J., Zhao, Y., Nie, J., Chen, X., Wang, A., Liu, H., 2018. Autophagy regulates high concentrations of iodide-induced apoptosis in SH-SY5Y cells. Toxicol. Lett. 284, 129–135.
Zuba, D., Adamowicz, P., Byrska, B., 2013. Detection of buphedrone in biological and non-biological material-two case reports. Forensic Sci. Int. 227 (1–3), 15–20.
Zwartsen, A., Verboven, A.H.A., van Kleef, R., Wijnolts, F.M.J., Westerink, R.H.S., Hondebrink, L., 2017. Measuring inhibition of monoamine reuptake transporters by new psychoactive substances (NPS) in real-time using a high-throughput, fluorescence-based assay. Toxicol. In Vitro 45 (Pt 1), 60–71.